www.coinweb.no

SINTEF Building and Infrastructure Anja B. E. Klausen and Øyvind Bjøntegaard (NPRA)

Temperature Development in On-Site Curing Boxes

COIN Project report 54 – 2014

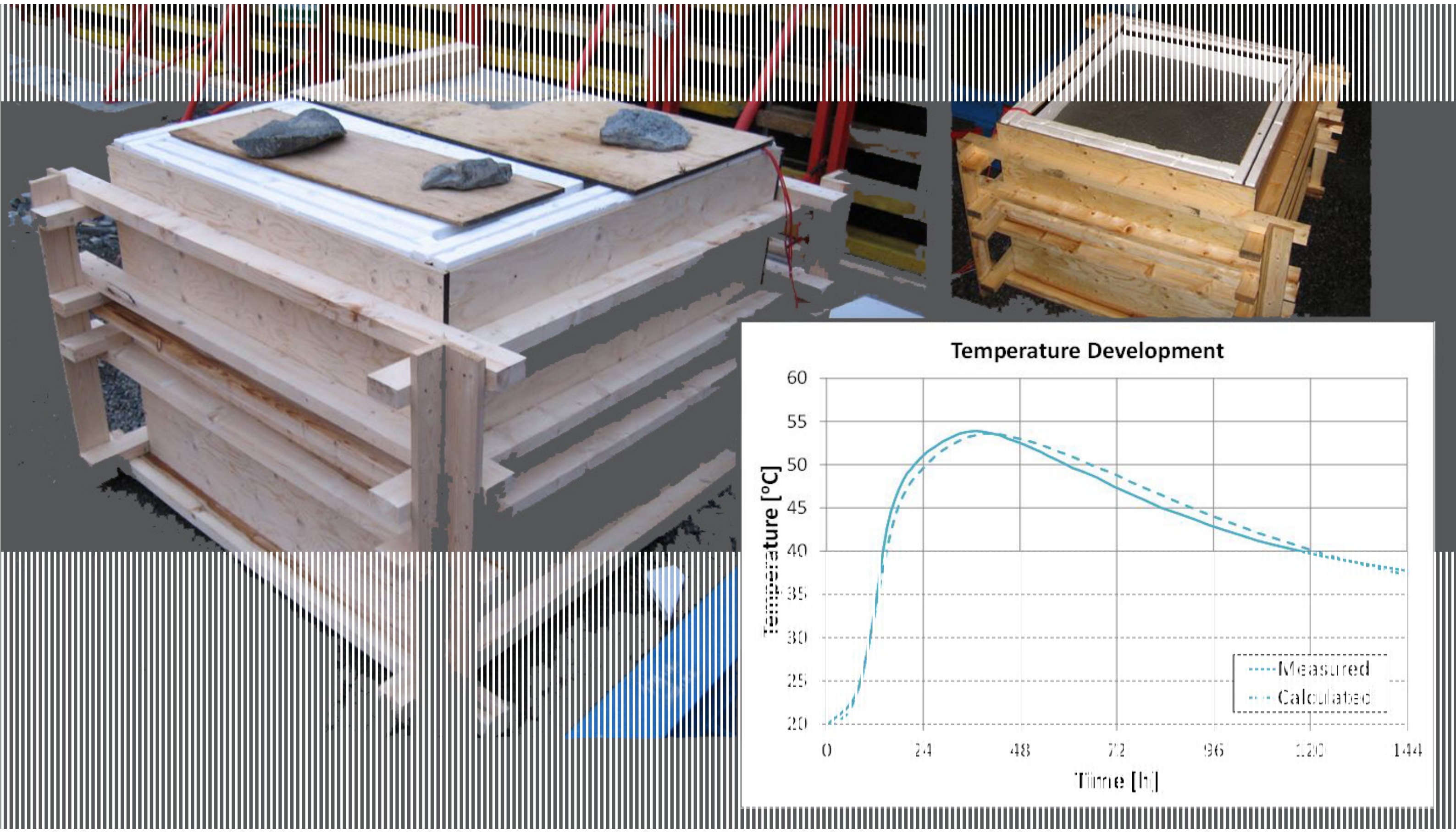

SINTEF Building and Infrastructure

Anja B. E. Klausen and Øyvind Bjøntegaard (NPRA)

Temperature Development in On-Site Curing Boxes

Technical performance

SP 3.1 Crack free concrete structures

COIN Project report 54 – 2014

COIN Project report no 54
Anja B. E. Klausen and Øyvind Bjøntegaard (NPRA)
Temperature Development in On-Site Curing Boxes
Technical performance
SP 3.1 Crack free concrete structures

Keywords:
Crack-free concrete, Hydration heat, concrete curing box tests

Project no.: 102000442-6

Photo, cover: «On-Site Curing Box», SINTEF Building and Infrastructure

ISSN 1891–1978 (online)
ISBN 978-82-536-1429-8 (pdf)

Address: Forskningsveien 3 B
POBox 124 Blindern
N-0314 OSLO
Tel: +47 22 96 55 55
Fax: +47 22 69 94 38 and 22 96 55 08

www.sintef.no/byggforsk
www.coinweb.no

Cooperation partners / Consortium Concrete Innovation Centre (COIN)

Kværner Engineering
Contact: Jan-Diederik Advocaat
Email: Jan-Diederik.Advocaat@kvaerner.com
Tel: +47 67595050

Saint Gobain Weber
Contact: Geir Norden
Email: geir.norden@saint-gobain.com
Tel: +47 22887700

Norcem AS
Contact: Terje Rønning
Email: terje.ronning@norcem.no
Tel: +47 35572000

NTNU
Contact: Terje Kanstad
Email: terje.kanstad@ntnu.no
Tel: +47 73594700

Mapei AS
Contact: Trond Hagerud
Email: trond.hagerud@mapei.no
Tel: +47 69972000

SINTEF Building and Infrastructure
Contact: Tor Arne Hammer
Email: tor.hammer@sintef.no
Tel: +47 73596856

Skanska Norge AS
Contact: Sverre Smeplass
Email: sverre.smeplass@skanska.no
Tel: +47 40013660

Norwegian Public Roads Administration
Contact: Kjersti K. Dunham
Email: kjersti.kvalheim.dunham@vegvesen.no
Tel: +47 22073940

Unicon AS
Contact: Stein Tosterud
Email: stto@unicon.no
Tel: +47 22309035

Veidekke Entreprenør ASA
Contact: Christine Hauck
Email: christine.hauck@veidekke.no
Tel: +47 21055000

Preface

This study has been carried out within COIN - Concrete Innovation Centre - one of presently 14 Centres for Research based Innovation (CRI), which is an initiative by the Research Council of Norway. The main objective for the CRIs is to enhance the capability of the business sector to innovate by focusing on long-term research based on forging close alliances between research-intensive enterprises and prominent research groups.

The vision of COIN is creation of more attractive concrete buildings and constructions. Attractiveness implies aesthetics, functionality, sustainability, energy efficiency, indoor climate, industrialized construction, improved work environment, and cost efficiency during the whole service life. The primary goal is to fulfil this vision by bringing the development a major leap forward by more fundamental understanding of the mechanisms in order to develop advanced materials, efficient construction techniques and new design concepts combined with more environmentally friendly material production.

The corporate partners are leading multinational companies in the cement and building industry and the aim of COIN is to increase their value creation and strengthen their research activities in Norway. Our over-all ambition is to establish COIN as the display window for concrete innovation in Europe.

About 25 researchers from SINTEF (host), the Norwegian University of Science and Technology - NTNU (research partner) and industry partners, 15 - 20 PhD-students, 5 - 10 MSc-students every year and a number of international guest researchers, work on presently eight projects in three focus areas:

- Environmentally friendly concrete
- Economically competitive construction
- Aesthetic and technical performance

COIN has presently a budget of NOK 200 mill over 8 years (from 2007), and is financed by the Research Council of Norway (approx. 40 %), industrial partners (approx 45 %) and by SINTEF Building and Infrastructure and NTNU (in all approx 15 %).

For more information, see www.coinweb.no

Tor Arne Hammer
Centre Manager

Summary

Reducing the risk of through-cracking in mass concrete during the hardening phase is mainly a question of reducing the hydration heat and, thus, reducing the temperature-increase in a hardening concrete member restrained against movement. The report deals with on-site curing box tests and gives some data on what to expect with regard to hydration heat and temperature increase when testing a concrete with a certain composition in future tests.

A series of FEM-analyses were run in DIANA, and the temperature developments for a various set of concretes, curing box designs as well as ambient conditions were evaluated. The main result for each analysis is given as the maximum temperature increase (ΔT_{max}) in the core of the curing box. The majority of analyses have been based on data for four concretes; *ANL FA, ANL FA + 8FA, ANL FA + 16FA and Ready-mix 1 (50FA)* with a fly ash content of 19 %, 27 %, 35 % and 50 %, respectively. It was found that when increasing the size of the curing box, ΔT_{max} increases, i.e. the temperature development sensitivity with regards to the surrounding conditions decreases. This effect is more pronounced the lower the ambient temperature. Likewise, the same effect is obtained by increasing the insulation thickness. The effect of wind speed was also investigated, and it was found that the effect of 0 and 5 m/s wind is insignificant regardless of the given curing box sizes and insulation thicknesses.

An extended series of temperature development analyses, with a variation of temperature conditions and curing boxes, were run for *ANL FA + 16FA*. For all studied curing box alternatives, there seems to be an approximately linear correlation between ΔT_{max} and ambient temperature, where the slope of the trend line represents the curing box's sensitivity to the surrounding conditions. Among the studied curing box alternatives it is found, for instance, that the sensitivity of ΔT_{max} to the ambient temperature is about the same for a 0.2 m^3 curing box with 200 mm insulation and for a 1.0 m^3 curing box with 100 mm insulation. As expected, the largest 1.0 m^3 curing box with 200 mm insulation has the lowest sensitivity due to the ambient conditions, but there is still a difference of 5 ^oC in ΔT_{max} between the two extreme ambient temperature cases T = -15 ^oC and T = 30 ^oC. Hence, even when using the curing box with the least temperature sensitivity, it is still necessary to consider the ambient temperature. It can be debated whether one curing box is more favourable than the other, as all seem to have an approximately linear correlation between ΔT_{max} and ambient temperature, and, thus, the ambient conditions can in principle be corrected for in all cases.

An extended series of analyses, with a variety of ambient temperatures and initial concrete temperatures, was conducted for the defined curing box reference case, *Size* = 1.0 m^3, $t_{insulation}$ = 100 mm, v = 0 m/s. The results show a rather linear correlation between ΔT_{max} and ambient temperature. One linear model for ΔT_{max} versus ambient temperature was established. The model gives good agreement with the analysis results for the concretes in question.

In addition, more as a curiosity, a series of analyses were performed with the aim to find out what wall thicknesses give a ΔT_{max} that is approximately equivalent to that of the various curing boxes with 100 mm insulation thicknesses. The results indicate that curing boxes with size 1.00 m^3, 0.51 m^3 and 0.22 m^3 represent wall thicknesses of about 1500 mm, 1300 mm, and 1100 mm, respectively. These are approximate numbers, as it was also found that the relation to some extend was dependent on the hydration heat characteristics of the concrete.

Table of contents

1 Introduction

1.1 Background

The temperature development of a given concrete can be measured in a curing box (a so-called semi-adiabatic calorimeter). Relatively small curing boxes are generally used in the laboratory (indoor). Curing boxes with different sizes have been used on-site (outdoor), and the most frequent one has been a box with net concrete volume of 1.0 m^3 (1.0 x 1.0 x 1.0 m) surrounded by insulation with thickness t = 100 mm.

For contractors and others doing on-site curing box tests in order to map out concretes with the aim to find a concrete composition for low-heat purposes, it would be convenient with a quick guideline on what to expect with regard to temperatures and heat developments. For this purpose, the present report gives some numbers on what could be expected as measured temperatures during on-site curing box tests, as well as on adiabatic temperature/heat developments. The effect of curing box size and degree of insulation has been studied, as well as the effect of concrete type (among some previously tested concretes consisting of fly ash or slag as part of the binder). By running a series of FEM-analyses in DIANA, the temperature developments for a various set of concretes, curing box designs as well as ambient conditions are evaluated.

The main concern in this context is to limit/avoid through-cracks during the hardening phase of massive structures due to restraint from adjoining structures / cold casting joints. Lowering the hydration heat generated temperature increase of the concrete is a powerful tool to achieve this. We know however that temperature is only one of several properties that govern cracking, but temperature (producing thermal dilation) is generally the predominant factor. Temperature is easy to measure and evaluate, and therefore often used alone as a simplified, but still very useful, requirement for crack limitation. More accurate evaluation of cracking risk (i.e. stress-based curing technology) requires a far more comprehensive approach; this is not the scope of the present report.

1.2 Objectives

The main objective is, by 3D simulations, to investigate various on-site curing box alternatives (size, insulation) and their sensitivity to the ambient conditions. The simulations make use of experimental data for different concretes with varying degree of «low-heat» properties, i.e. both the rate of heat generation and the final heat vary greatly among the previously tested concretes. Results from future on-site curing box tests may be compared to the numbers presented here.

2 Case description

2.1 Materials

The majority of analyses have been based on data for four concretes, having different contents of fly ash (FA). The name given to the concretes are listed below, and their composition (and total FA-content) is given in Table 2.1.

- *ANL FA*
- *ANL FA + 8FA*
- *ANL FA + 16FA*
- *Ready-mix 1 (50FA)*

Table 2.1 Mix design and FA-content of current concretes

	ANL FA [kg/m^3]	**ANL FA + 8FA** [kg/m^3]	**ANL FA + 16FA** [kg/m^3]	**Ready-mix 1 (50FA)** [kg/m3]
Cement	368.9	327.4	287.1	190.0
FA_{cem}	69.0	61.2	53.7	38.0
FA_{added}	0	36.4	71.8	114.0
Silica	18.4	18.2	17.8	15.0
Free water	162.3	160.0	157.8	135.5
Sand 0-8	1211.1	1211.1	1211.1	950.0
Gravel 8-16	611.5	611.5	611.5	310.0
Gravel 16-32	0	0	0	620.0
Admixture	2.03	1.80	1.58	7.5
Total FA-content, FA/(c+FA)*)	**19**	**27**	**35**	**50**

*) The FA-content for each concrete is calculated by the following formula:

$$FA\ content = \frac{FA_{cem} + FA_{added}}{(FA_{cem} + FA_{added} + Cement)} \cdot 100\ \%$$

Three of the concretes above, *ANL FA, ANL FA + 8FA* and *ANL FA + 16FA*, have recently been investigated within the COIN project «COIN FA3.1 Crack Free Concrete Structures». The adiabatic temperature development data and the material parameters applied in the present analyses are extracted from [Kjellmark et al.; 2013].

The concrete *Ready-mix 1 (50FA)* was used and tested experimentally while building the «Møllenberg Tunnel» in Trondheim, [Statens Vegvesen; 2013] and [SINTEF test report; 2011]. The adiabatic temperature development data and material parameters applied in the present analyses are taken from that experimental work.

In addition, data for a 70 % slag concrete named *Ready-mix 2 (70slag)* was received from [Kristiansen; 2013], and included into the analyses at a late stage. *Ready-mix 2 (70slag)* mix design and material parameters are presented in Appendix C.

The material parameters that have been used for each concrete in the analysis are presented in Section 3.

2.2 Analysis and Models Construction

Curing box heat development analyses for a wide set of input and material parameters are performed. The varying parameters are as follows:

Concrete
The current analyses are performed with four different concretes, Section 2.1:
- *ANL FA (19 % FA)*
- *ANL FA + 8FA (27 % FA)*
- *ANL FA + 16FA (35 % FA)*
- *Ready-mix 1 (50FA) (50 % FA)*

Curing box size
Three different curing box sizes are defined and applied the analyses:
- 1000 x 1000 x 1000 mm = 1.000 m^3
- 800 x 800 x 800 mm = 0.512 m^3
- 600 x 600 x 600 mm = 0.216 m^3

Insulation thickness
Each curing box size is analysed with two different insulation thicknesses:
- t = 100 mm
- t = 200 mm

Ambient temperature
Three different ambient temperatures representing summer, spring/fall and winter are used:
- Summer: T = 20 °C
- Spring/fall: T = 5 °C
- Winter: T = -10 °C

Wind
The analyses are run with two different wind speeds:
- v = 0 m/s
- v = 5 m/s

The wide range of varying parameters results in a considerable amount of analyses to be run. For an overview, a matrix displaying the required analyses to be run for each concrete is presented in Table 2.2.

The calculation matrix presented in Table 2.2 shows that the chosen parameter variation requires as much as 36 analyses for each of the four main concretes. The concrete *Ready-mix 1 (50FA)* was analysed first, and its results indicated that the wind speed does not have a significant impact on the temperature development for the various cases, see Section 4.2.5. Hence, the three remaining concretes were analysed with a wind speed *v = 0 m/s* only, which reduced the amount of analyses by 50 %.

Table 2.2 Parameter variation for each concrete

Size [m³]	**Insulation** [mm]	**Wind** [m/s]	**Temperature** [°C]	**Name**
1.000	100	0	-10	*concrete_1_10_0_10*
			5	*concrete_1_10_0_5*
			20	*concrete_1_10_0_20*
		5	-10	*concrete_1_10_5_10*
			5	*concrete_1_10_5_5*
			20	*concrete_1_10_5_20*
	200	0	-10	*concrete_1_20_0_10*
			5	*concrete_1_20_0_5*
			20	*concrete_1_20_0_20*
		5	-10	*concrete_1_20_5_10*
			5	*concrete_1_20_5_5*
			20	*concrete_1_20_5_20*
0.512	100	0	-10	*concrete_05_10_0_10*
			5	*concrete_05_10_0_5*
			20	*concrete_05_10_0_20*
		5	-10	*concrete_05_10_5_10*
			5	*concrete_05_10_5_5*
			20	*concrete_05_10_5_20*
	200	0	-10	*concrete_05_20_0_10*
			5	*concrete_05_20_0_5*
			20	*concrete_05_20_0_20*
		5	-10	*concrete_05_20_5_10*
			5	*concrete_05_20_5_5*
			20	*concrete_05_20_5_20*
0.216	100	0	-10	*concrete_022_10_0_10*
			5	*concrete_022_10_0_5*
			20	*concrete_022_10_0_20*
		5	-10	*concrete_022_10_5_10*
			5	*concrete_022_10_5_5*
			20	*concrete_022_10_5_20*
	200	0	-10	*concrete_022_20_0_10*
			5	*concrete_022_20_0_5*
			20	*concrete_022_20_0_20*
		5	-10	*concrete_022_20_5_10*
			5	*concrete_022_20_5_5*
			20	*concrete_022_20_5_20*

The case «*Size* = *1.0* m^3, $t_{insulation}$ = *100 mm, v = 0 m/s*» is considered the reference case, since such curing box has already been made on-site several times. For each of the five concretes presented in Section 2.1, heat development analyses with a variety of ambient temperatures and initial concrete temperatures were run for the reference case, trying to establish a relation between heat development and ambient temperature.

In addition, more as a curiosity, a series of analyses were performed with the aim to find out approximately what wall thickness each curing box variant represent (assuming normal plywood as formwork and average temperature for the wall), see Section 4.4.

3 DIANA model

3.1 Geometry

The geometry and measurements of the three different sizes of curing boxes applied in the current Diana analyses are shown in Figure 3.1.

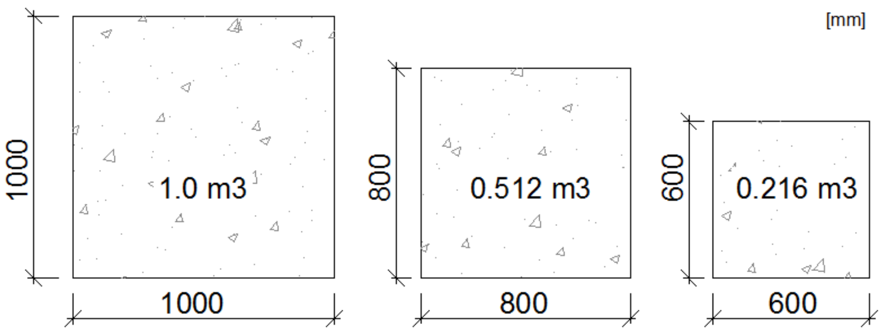

Figure 3.1 Curing boxes – geometry and measurements

3.2 Finite element model and finite elements

3.2.1 Finite element model

The desired output for each analysis is the nodal temperature in the centre of the specimen. Each cube side is divided in four elements. Hence, the element sizes are 250 mm x 250 mm x 250 mm, 200 mm x 200 mm x 200 mm and 150 mm x 150 mm x 150 mm for curing boxes 1.0 m^3, 0.512 m^3 and 0.216 m^3, respectively.

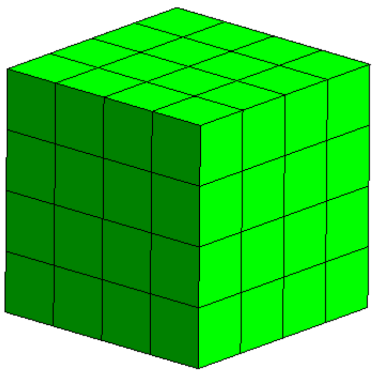

Figure 3.2 Curing box – Finite element model

A series of analyses applied a curing box model with a finer mesh, 8 x 8 x 8 elements, were also performed, confirming that the chosen 4 x 4 x 4 mesh gives sufficient accuracy.

3.2.2 Finite elements

In the current analyses, two different types of elements are used.

The flow element HX8HT, an eight-node isoparametric brick element, is used for the general three-dimensional potential flow analysis, Figure 3.3. HX8HT is based on linear interpolation and Gauss integration [TNO DIANA BV, 2010].

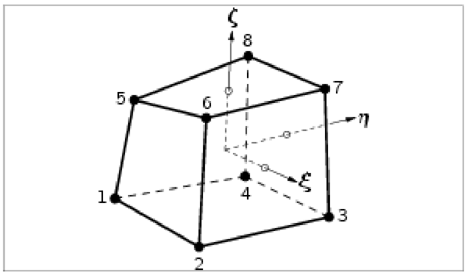

Figure 3.3 HX8HT, flow element, brick, 8 nodes [TNO DIANA BV, 2010]

To describe the heat convection along the outside surfaces of the concrete structure, the flow element BQ4HT is used, Figure 3.4 [TNO DIANA BV, 2010].

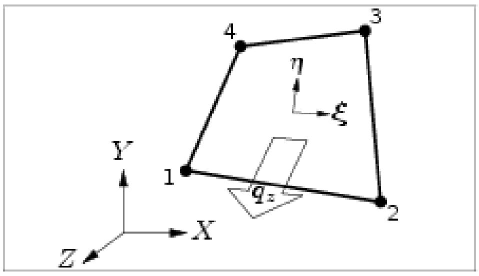

Figure 3.4 BQ4HT, flow element, quadrilateral boundary, 4 nodes [TNO DIANA BV, 2010]

3.3 Boundary conditions

3.3.1 Temperature

The initial concrete temperature as delivered to a working site depends on seasonable variations in the ambient temperature; the assumed relation is given in Table 3.1.

Table 3.1 Applied temperature presumptions

	Ambient temperature [^oC]	Initial concrete temperature [^oC]
Summer	20	20
Spring/fall	5	18
Winter	-10	15

The convection of the boundary elements are implemented into the model through the modelling of the material properties, Section 3.4.

3.3.2 Boundary constraints

The current analyses consist of flow analyses merely, and thus the boundary constraints are of no significance for the obtained results. The applied boundary constraints are shown in Figure 3.5.

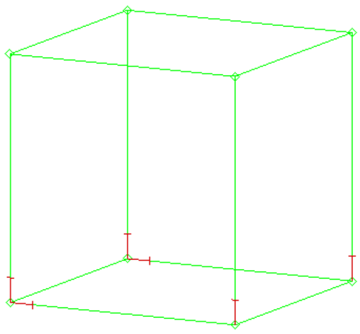

Figure 3.5 Curing box – boundary constraints

3.4 Material models

3.4.1 Concrete materials coefficients

The concretes are modelled as fresh/hardening concrete in the analyses. The applied material parameters for the different concretes are given in Table 3.2. Material parameters for the additional slag concrete *Ready-mix 2 (70slag)* are given in Appendix C.

Table 3.2 Material coefficients used in the analyses

		Concrete			
		ANL FA	**ANL FA + 8FA**	**ANL FA + 16FA**	**Ready-mix 1 (50FA)**
Density	[kg/m^3]	2 390	2 380	2 380	2 375
Th. conductivity	[W/mK]	2.2	2.2	2.2	2.2
Heat capacity	[kJ/m^{3}K]	2 414	2 404	2 404	2 446
Arrhenius*$^{)}$	[K]	3 791	3 954	4 380	4 210
Adiabatic temperature development		Figure 3.7	Figure 3.7	Figure 3.7	Figure 3.7

$^{*)}$ The Arrhenius constant is the activation energy divided by the gas constant. It is constant for all temperatures, and based on the activation energy valid for $\geq 20\,^oC$

The previously described DIANA model and the defined material parameters, Table 3.2, were calibrated and confirmed in the following way: The adiabatic temperature developments for the given concretes were found from actual curing box tests. Furthermore, the actual curing boxes and ambient conditions used in the various tests were modelled in DIANA as previously described. These «back-calculated temperature developments» for the various curing box tests give relatively good agreement with each test result, see Figure 3.6. Hence, this shows that relevant values for convection- and conductivity properties have been implemented in the DIANA-analyses.

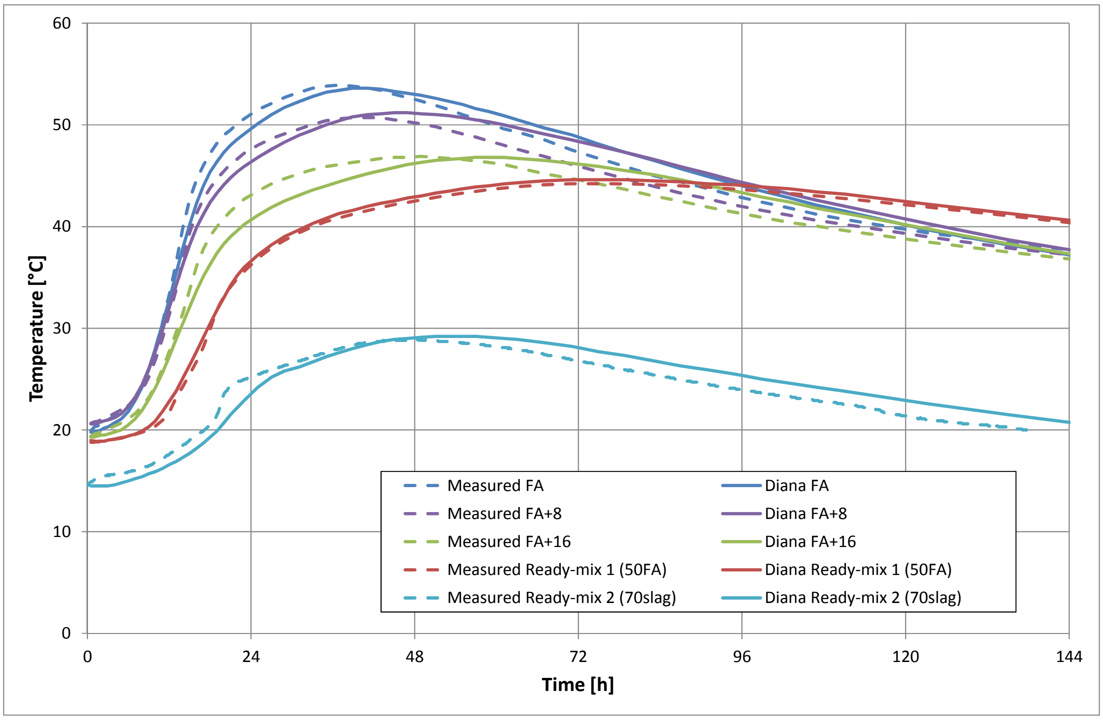

Figure 3.6 Measured temperature and back-calculated temperature with time

The adiabatic temperature developments are extracted from experiments and presented in Figure 3.7 (and Appendix B) for all given concretes.

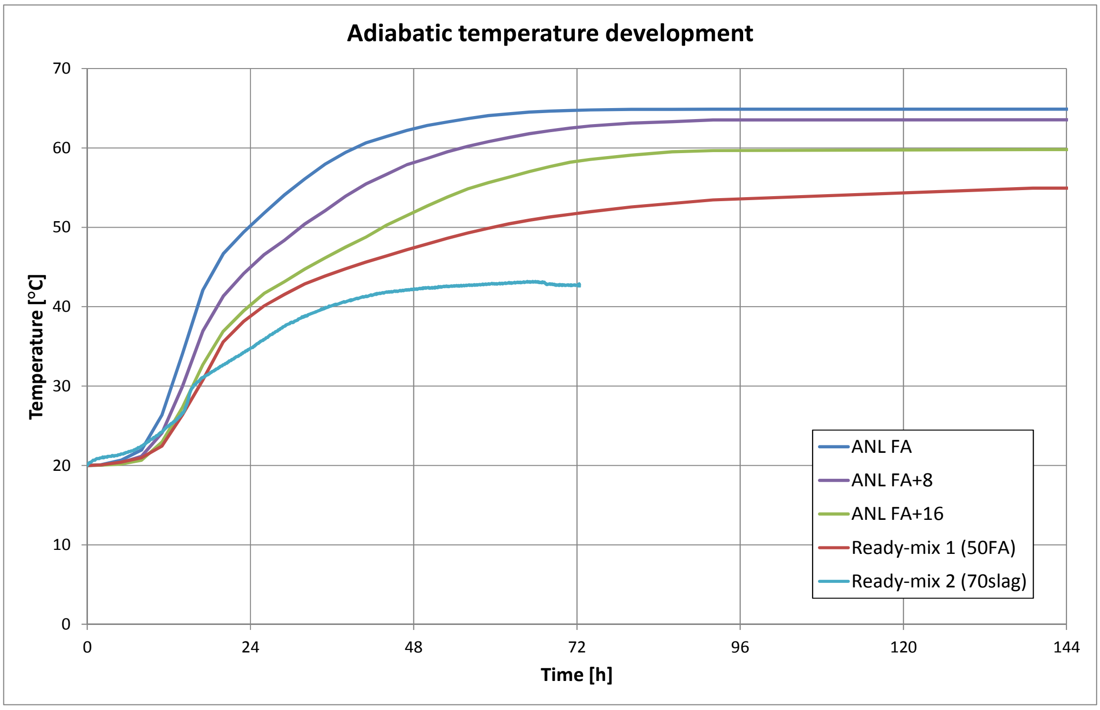

Figure 3.7 Adiabatic temperature developments

The adiabatic temperature developments presented in Figure 3.7 are converted into isothermal heat development [*kJ/ kg cem + s + FA + slag*] and presented in Figure 3.8.

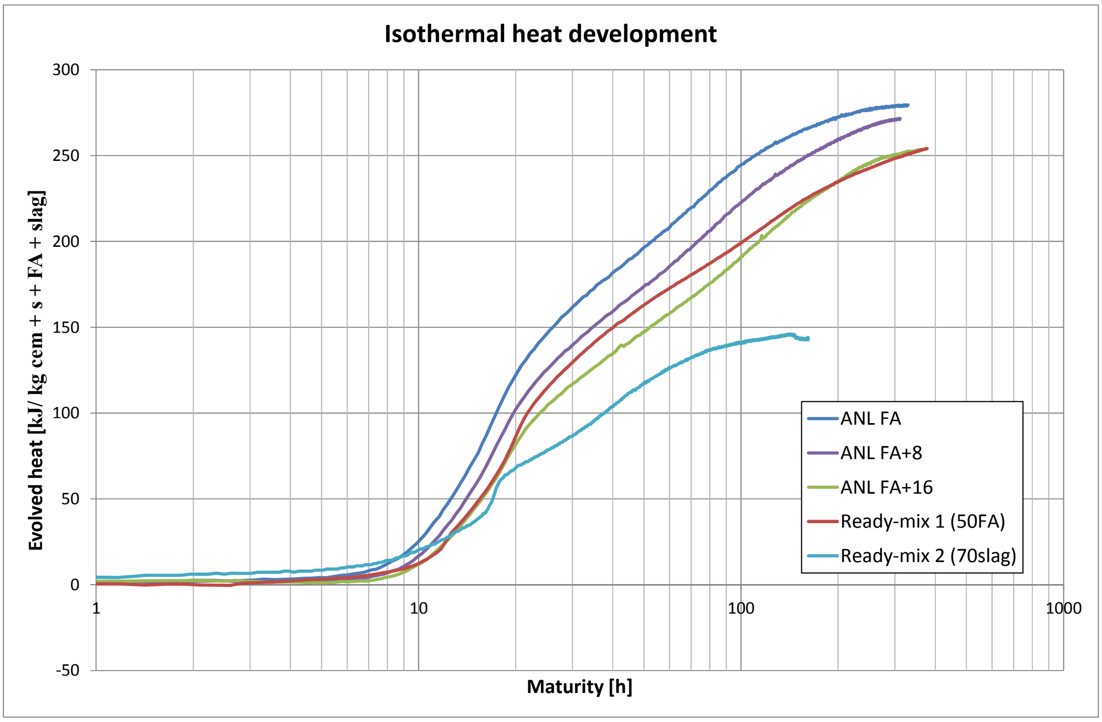

Figure 3.8 Isothermal heat development

3.4.2 Boundary elements

Various material models are established, representing the boundary convection for the different predefined cases. The applied convection coefficients for the boundaries in question are calculated in Appendix A and presented in Table 3.3.

Table 3.3 Convection coefficients for the concrete boundaries

Convection coefficient [W/m^{2}K]		***Wind speed***	
		v = 0 m/s	*v = 5 m/s*
Insulation	*t = 100 mm*	0.312	0.326
	t = 200 mm	0.163	0.166

3.5 Wall

In the simulations of a wall, the same material parameters and material model as described previously are used, but with the following exceptions;

- The boundary convection in x- and y- direction is set to zero (modelling infinite length of the wall)
- The boundary convection in z-direction is set to 3.49 W/m^{2}K (representing plywood with a thickness t = 15 mm and wind speed v = 0 m/s)
- Ambient air temperature 20 $^{\circ}$C
- The thickness in z-direction (representing the wall thickness) is changed until the desired maximum temperature increase is obtained

4 Results

4.1 Introduction

The DIANA temperature development results for the four main concretes are presented in Section 4.2, while the results from the extended analysis matrix for the reference case are presented and discussed in Section 4.3.

The wall simulations are presented in Section 4.4.

4.2 Temperature developments

4.2.1 Introduction

The main result for each analysis is given as the maximum temperature increase (ΔT_{max}) in the core of the curing box, see illustration in Figure 4.1.

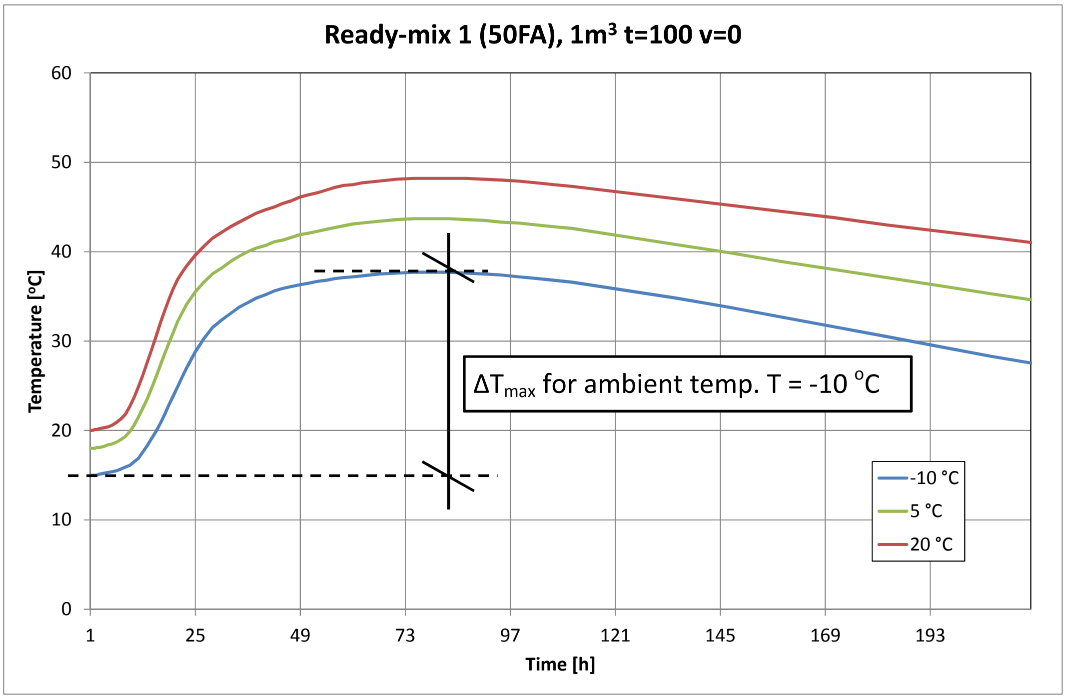

Figure 4.1 Maximum temperature increase ΔT_{max}, which is the basis for the evaluation

First, the different ΔT_{max} results for each concrete are presented by tables and charts in Section 4.2.2 – 4.2.5, thereafter the results are discussed in Section 4.2.6.

The concrete *Ready-mix 1 (50FA)* was analysed first, and the results indicated that the wind speed does not have a significant impact on the heat development in the defined curing boxes, see Section 4.2.5. Hence, the three remaining concretes were analysed with a wind speed v = 0 m/s only, Section 4.2.2 – 4.2.4.

4.2.2 ANL FA

Obtained ΔT_{max} results for *ANL FA* are presented in Table 4.1, and illustrated in Figure 4.2.

Table 4.1 Temperature developments, ANL FA

Size [m³]	**Insulation** [mm]	**Wind** [m/s]	**Temperature** [°C]	ΔT_{max} [°C]
1.00	100	0	-10	36.4
			5	38.6
			20	40.4
	200	0	-10	39.7
			5	41.1
			20	42.2
0.51	100	0	-10	34.0
			5	36.7
			20	38.9
	200	0	-10	38.2
			5	39.9
			20	41.3
0.22	100	0	-10	30.5
			5	34.0
			20	36.9
	200	0	-10	36.0
			5	38.1
			20	39.9

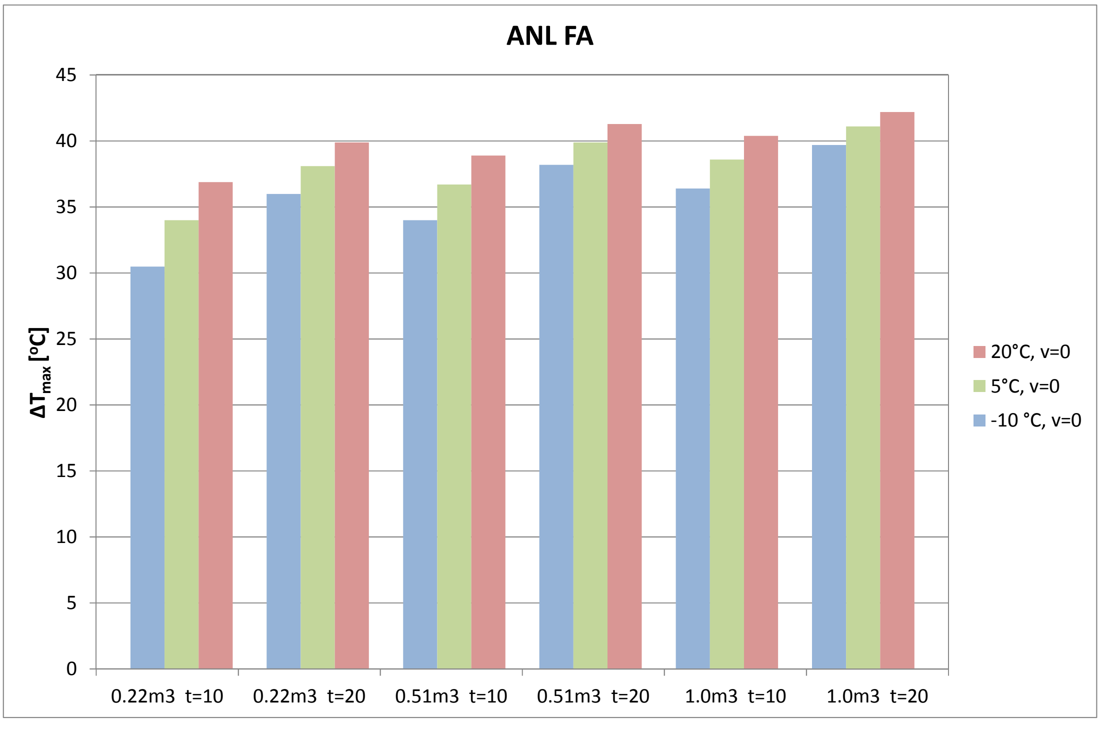

Figure 4.2 Temperature developments, ANL FA

4.2.3 ANL FA + 8 % FA

Obtained ΔT_{max} results for *ANL FA + 8FA* are presented in Table 4.2, and illustrated in Figure 4.3.

Table 4.2 Temperature developments, ANL FA + 8FA

Size [m³]	**Insulation** [mm]	**Wind** [m/s]	**Temperature** [°C]	*ΔT_{max}* [°C]
1.00	100	0	-10	32.7
			5	35.5
			20	37.8
	200	0	-10	37.0
			5	38.7
			20	40.1
0.51	100	0	-10	30.0
			5	33.3
			20	36.1
	200	0	-10	35.1
			5	37.3
			20	39.1
0.22	100	0	-10	26.1
			5	30.3
			20	33.9
	200	0	-10	32.5
			5	35.2
			20	37.5

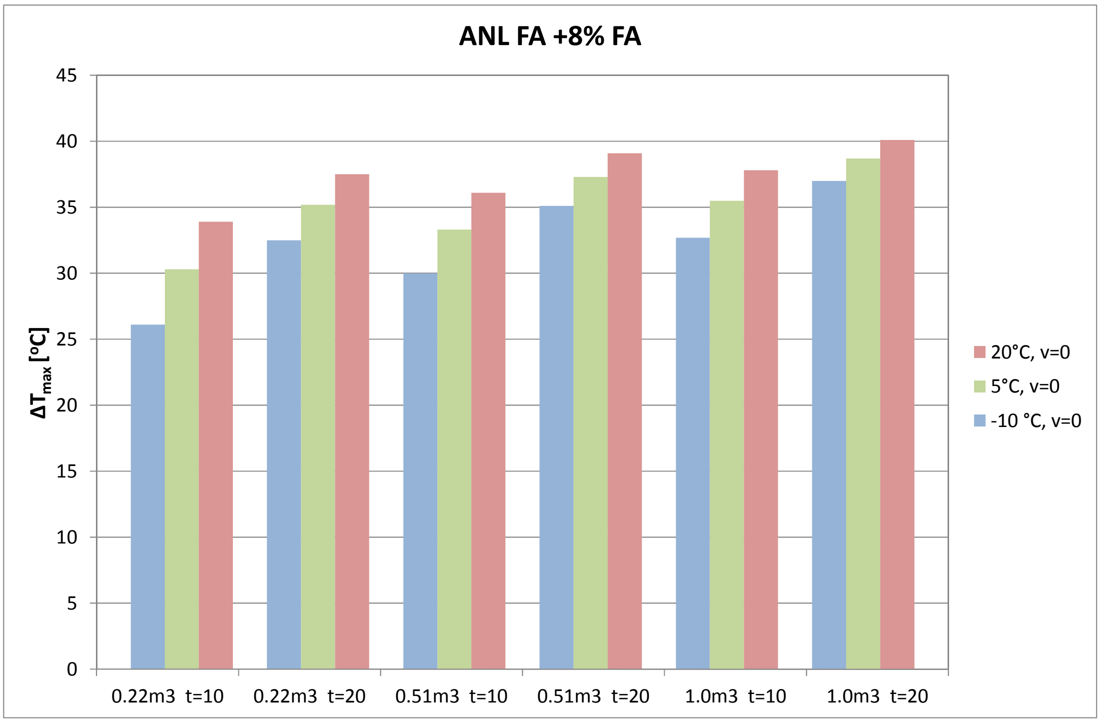

Figure 4.3 Temperature developments, ANL FA + 8FA

4.2.4 ANL FA + 16 % FA

Obtained ΔT_{max} results for *ANL FA + 16FA* are presented in Table 4.3, and illustrated in Figure 4.4.

Table 4.3 Temperature developments, ANL FA + 16FA

Size [m³]	**Insulation** [mm]	**Wind** [m/s]	**Temperature** [°C]	ΔT_{max} [°C]
1.00	100	0	-10	27.7
			5	31.3
			20	34.1
	200	0	-10	32.8
			5	34.9
			20	36.5
0.51	100	0	-10	24.6
			5	28.9
			20	32.5
	200	0	-10	30.8
			5	33.4
			20	35.4
0.22	100	0	-10	20.2
			5	25.6
			20	29.9
	200	0	-10	27.8
			5	31.3
			20	33.9

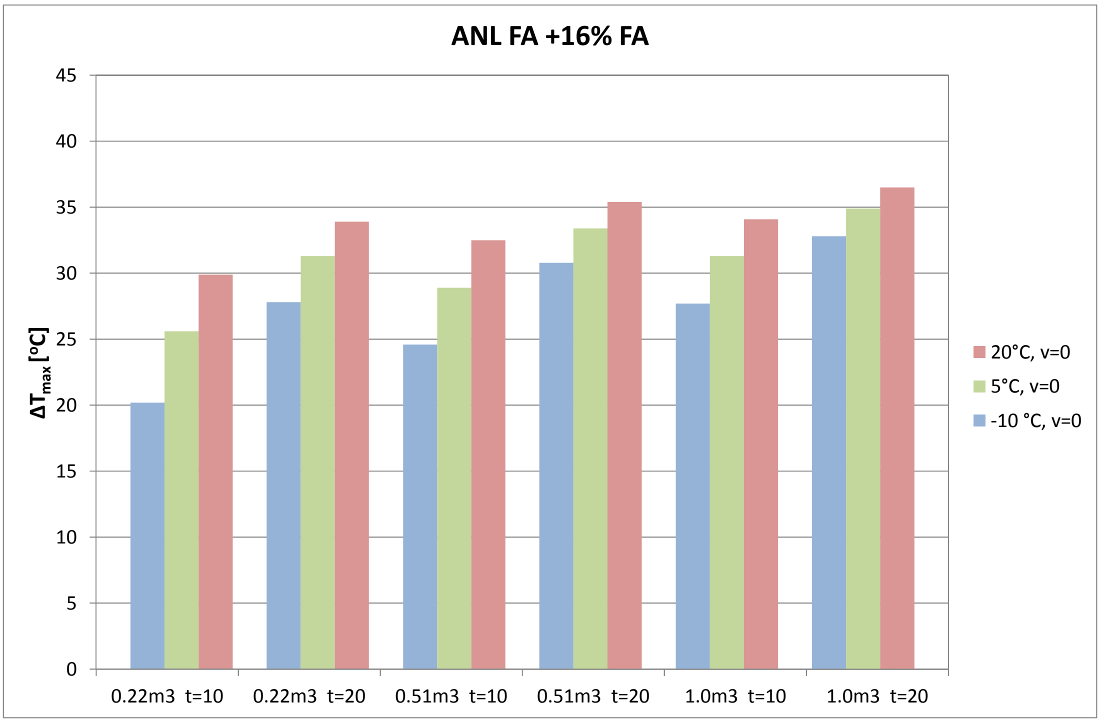

Figure 4.4 Temperature developments, ANL FA + 16FA

4.2.5 Ready-mix 1 (50FA)

Obtained ΔT_{max} results for the calculation cases defined in Table 2.2 for the concrete *Ready-mix 1 (50FA)* are presented in Table 4.4, and illustrated in Figure 4.5. Note that for this concrete, the effect of wind speed was investigated. It can be seen that the effect of 0 and 5 m/s wind is insignificant as the consequence on ΔT_{max} is limited to 0.3 ^{o}C, regardless of the given sizes and insulation thicknesses.

Table 4.4 Temperature developments, Ready-mix 1 (50FA)

Size [m^3]	**Insulation** [mm]	**Wind** [m/s]	**Temperature** [°C]	ΔT_{max} [°C]
1.00	100	0	-10	22.7
			5	25.7
			20	28.2
		5	-10	22.4
			5	25.5
			20	28.1
	200	0	-10	26.8
			5	28.8
			20	30.5
		5	-10	26.7
			5	28.7
			20	30.4
0.51	100	0	-10	20.2
			5	23.7
			20	26.8
		5	-10	19.9
			5	23.4
			20	26.6
	200	0	-10	25.1
			5	27.5
			20	29.5
		5	-10	25.0
			5	27.4
			20	29.4
0.22	100	0	-10	17.4
			5	21.0
			20	24.8
		5	-10	17.1
			5	20.7
			20	24.6
	200	0	-10	22.6
			5	25.6
			20	28.1
		5	-10	22.5
			5	25.4
			20	28.0

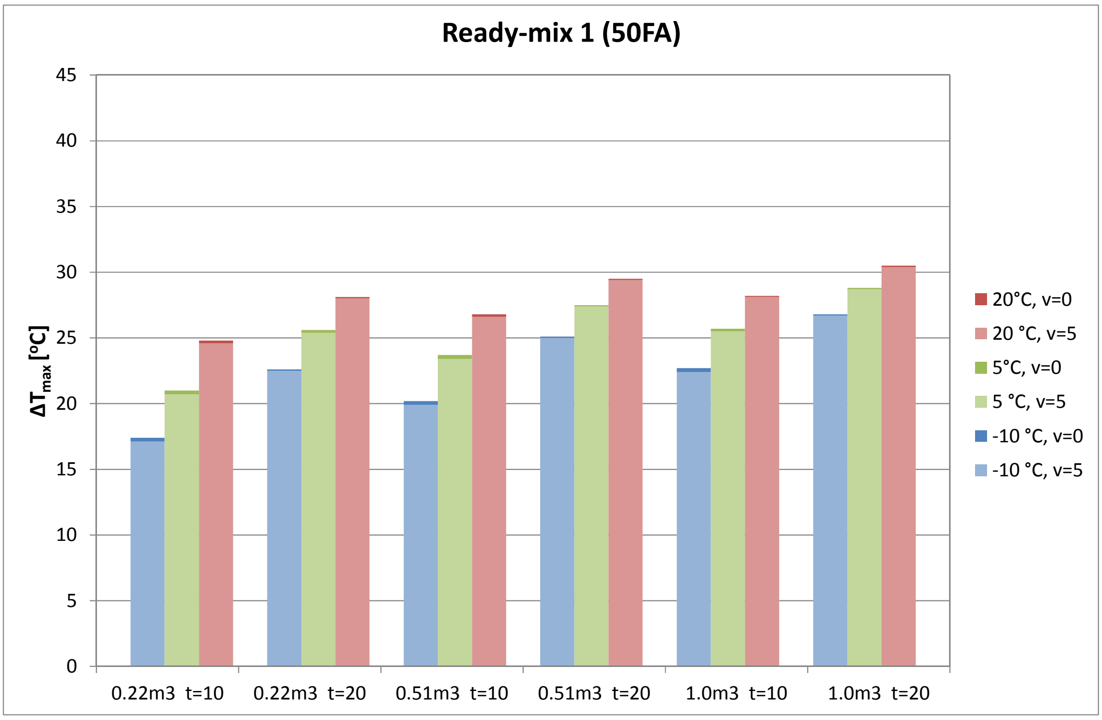

Figure 4.5 Temperature developments for Ready-mix 1 (50FA), also including the effect of wind speed 0 and 5 m/s

4.2.6 Discussion

The column chart presenting ΔT_{max} for *Ready-mix 1 (50FA)*, Figure 4.5, shows clearly that the wind speed only has a minor influence on the temperature development for the curing boxes in question. The consequence on ΔT_{max} is limited to 0.3 ^oC, regardless of the given sizes and insulation thicknesses. Hence, the remaining concretes were analysed for a wind speed $v = 0$ m/s only.

Figure 4.2 - Figure 4.5 show that when increasing the size of the curing box (and by that the concrete specimen), ΔT_{max} increases, and the sensitivity to the surrounding conditions decreases. This effect gets more pronounced at lower ambient temperature. Likewise, the same effect is obtained by increasing the insulation thickness. ΔT_{max} versus curing box size is illustrated in Figure 4.6 for the two studied insulation thicknesses; 100 mm and 200 mm. As can be seen, an exponential relationship is (vaguely) indicated – which would be expected as ΔT_{max} will approach the adiabatic temperature increase for an infinitely large curing box, regardless of insulation thickness.

A variation of temperature development analyses, with temperature conditions and curing boxes as given in Table 4.5, are run for *ANL FA + 16FA*. The results, hence the curing boxes' sensitivities to ambient temperature and initial concrete temperatures, are illustrated in Figure 4.7. For all curing boxes in question, there seems to be an approximately linear correlation between ΔT_{max} and ambient temperature, Figure 4.7. The slope of the trend line represents the curing box's sensitivity to the surrounding conditions. The flatter the trend line, the lower the curing box sensitivity. As can be seen from Figure 4.7, curing box 0.22 m^3 with insulation thickness t = 200 mm has approximately the same ambient temperature sensitivity as curing box 1.0 m^3 with insulation thickness t = 100 mm. As expected, the largest curing box with the thickest insulation, 1.0 m^3, t = 200 mm, has the lowest temperature sensitivity due to surrounding temperature conditions. There is still a difference of 5 ^oC in ΔT_{max} between the two extreme ambient temperature cases T = -15 ^oC and T = 30 ^oC. Hence, if using the curing box with the least temperature sensitivity still makes it necessary to consider the ambient temperature, it is debatable whether one of the curing boxes is more favourable than the others, as they all seem to have an approximately linear correlation between ΔT_{max} and ambient temperature.

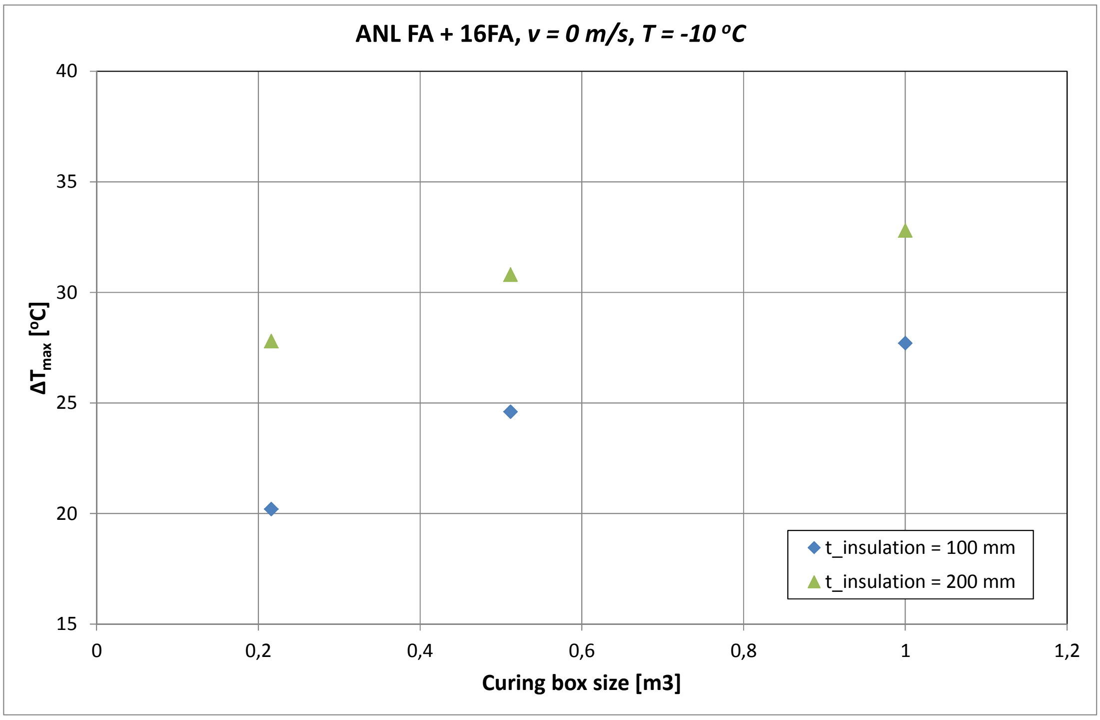

Figure 4.6 ΔT_{max} with curing box size, ANL FA + 16FA, initial concrete temp. 15 °C, T_{amb} = -10 °C

Table 4.5 ANL FA + 16FA: ΔT_{max} for a variation of curing boxes and ambient temperatures [°C]

Ambient temperature	**Initial concrete temperature**	**ΔT_{max}**					
		Size = 1.00 m^3		**Size = 0.51 m^3**		**Size = 0.22 m^3**	
		***t* = 100** [mm]	***t* = 200** [mm]	***t* = 100** [mm]	***t* = 200** [mm]	***t* = 100** [mm]	***t* = 200** [mm]
-15	12	25.7	31.6	22.2	29.3	17.7	25.9
-10	8	25.7	31.5	22.6	29.3	18.3	26.1
	15	27.7	32.8	24.6	30.8	20.2	27.8
5	18	31.3	34.9	28.9	33.4	25.6	31.3
20	20	34.1	36.5	32.5	35.4	29.9	33.9
30	22	35.7	37.4	34.4	36.6	32.6	35.4

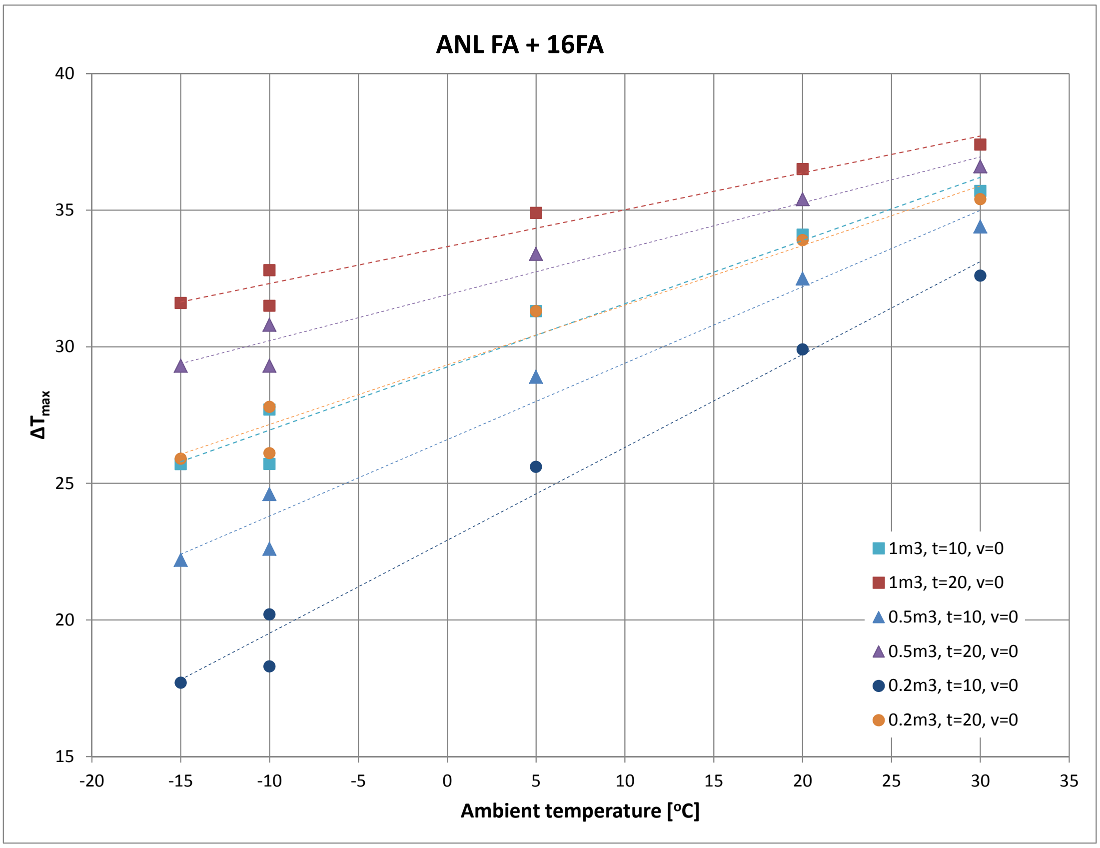

Figure 4.7 ΔT_{max} versus ambient temperature for ANL FA + 16FA

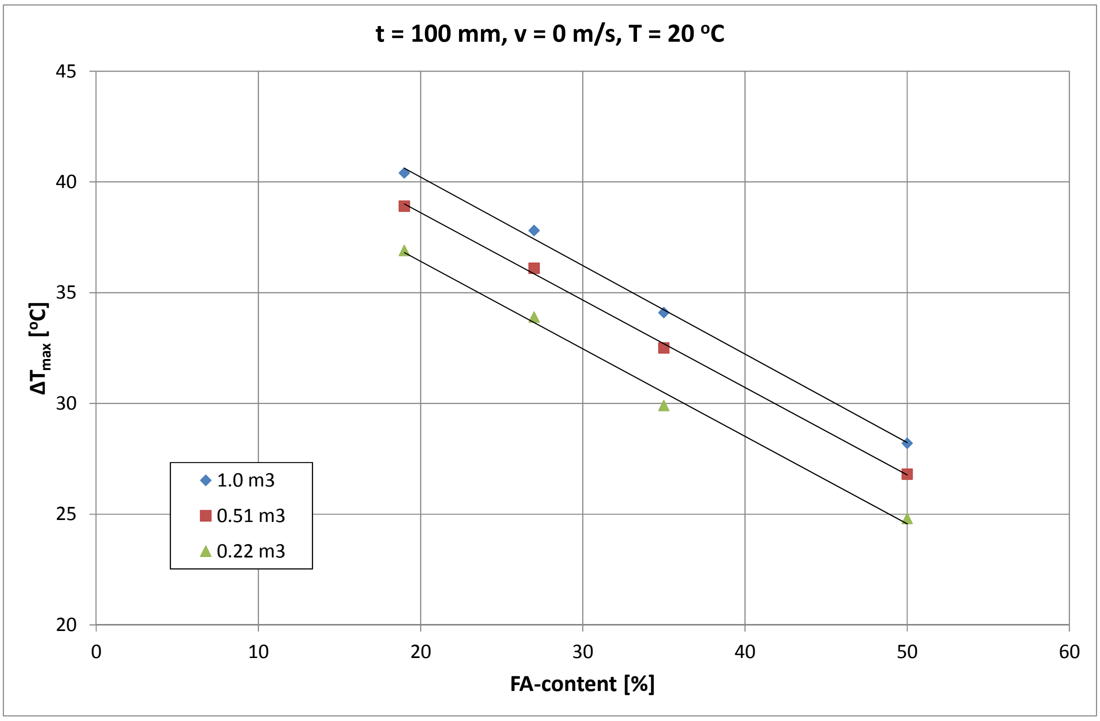

Figure 4.8 ΔT_{max} vs. FA-content for different curing box dimensions, ambient temperature $T = 20\,^oC$

The FA-content's influence on ΔT_{max} is illustrated in Figure 4.10. It can be seen that ΔT_{max} decreases with increasing FA-content. For high ambient temperatures, the correlation between ΔT_{max} and FA-content seems to be linear, but for low ambient temperatures it seems as if the correlation is non-linear.

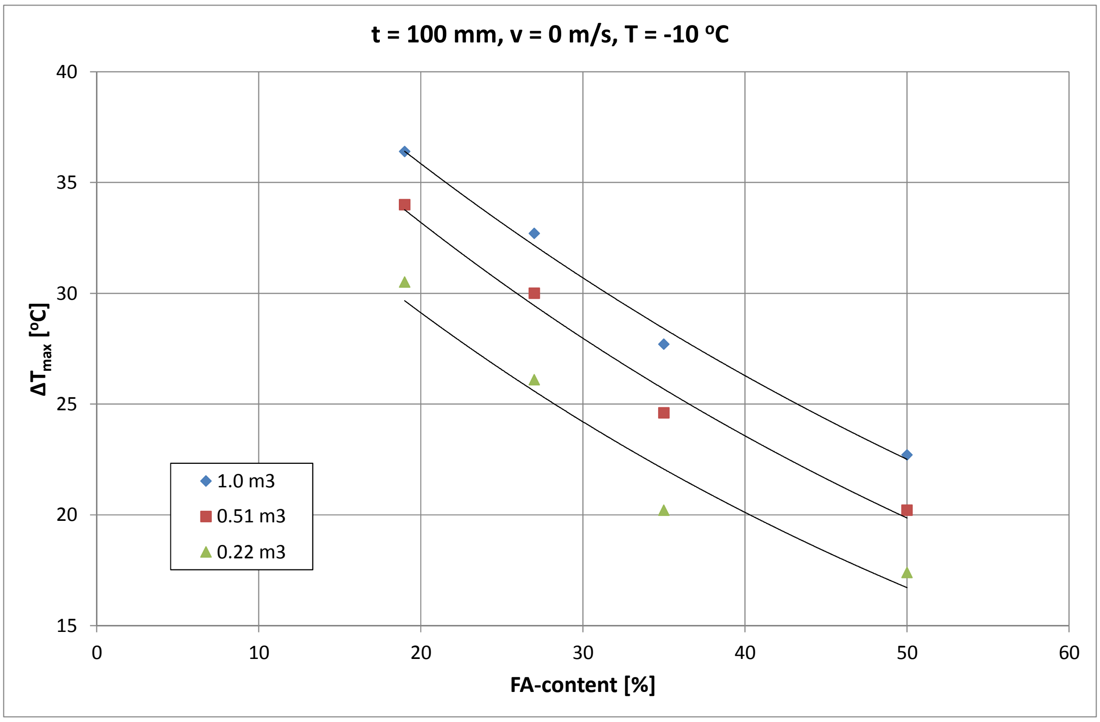

Figure 4.9 ΔT_{max} vs. FA-content for different curing box dimensions, ambient temperature T = -10 °C

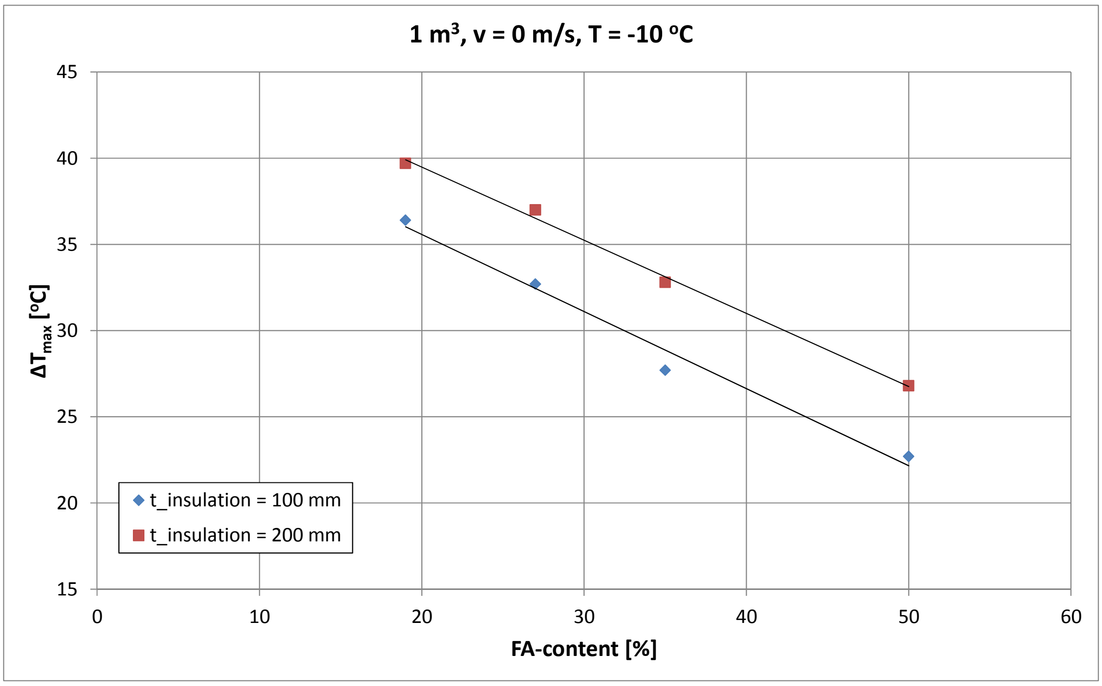

Figure 4.10 ΔT_{max} vs. FA-content for insulation thickness t = 100 mm and t = 200 mm, ambient temperature T = -10 °C

4.3 Reference case

An extended series of analyses, with a variety of surrounding temperatures and initial concrete temperatures, has been run for the curing box reference case: *Size = 1.0* m^3, $t_{insulation}$ *= 100 mm, v = 0 m/s*. The results are presented in Table 4.6 and Figure 4.11. Figure 4.11 clearly indicates a linear correlation between ΔT_{max} and ambient temperature, but with a small variation due to initial concrete temperature. Figure 4.11 in combination with Figure 4.7 indicates that an appurtenant linear correlation can be found for all given curing box variations.

Table 4.6 ΔT_{max} for the curing box reference case [°C]

Ambient temperature	Initial concrete temperature	ΔT_{max}				
		ANL FA	**ANL FA + 8FA**	**ANL FA + 16FA**	**Ready-mix 1 (50FA)**	**Ready-mix 2 (70slag)**
-15.0	5	33.8	29.5	23.4	19.7	15.4
	12	35.1	31.1	25.7	21.1	16.4
-10.0	8	35.2	31.3	25.7	21.3	–
	15	36.4	32.7	27.7	22.7	17.5
-2.5	8	36.5	32.9	27.8	23.1	18.0
	10	–	–	28.2	23.3	–
	12	–	–	28.6	23.6	–
	14	–	–	29.0	23.9	–
	16	–	–	29.5	24.2	–
	18	37.8	34.4	30.0	24.5	18.7
5.0	15	38.3	35.1	30.9	25.4	–
	18	38.6	35.5	31.3	25.7	19.4
	20	38.8	35.8	31.7	25.9	–
12.5	15	39.2	36.4	32.4	26.8	–
	19	39.5	36.7	32.8	27.0	20.2
20.0	20	40.4	37.8	34.1	28.2	21.0
30.0	22	41.5	39.2	35.7	29.8	21.9
	30	41.7	39.5	36.0	29.9	21.8

In Figure 4.12, the results from Figure 4.11 and Table 4.6 are converted into relative temperature developments by dividing each concrete's ΔT_{max} trend line by its ΔT_{max} at a surrounding temperature of $T = 20$ °C. Figure 4.12 shows that there is a small variation in the trend line slopes for the given concretes. This indicates that the curing box's sensitivity is dependent on the heat properties of the given concrete.

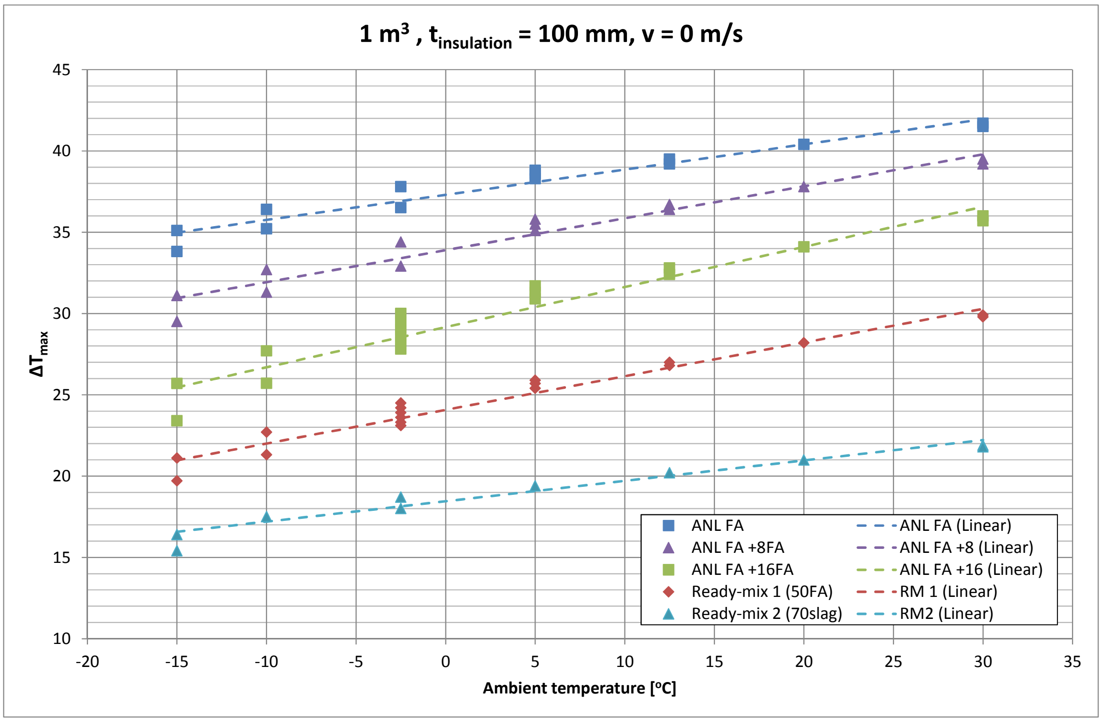

Figure 4.11 ΔT_{max} versus ambient temperature, with a variety of initial concrete temperatures

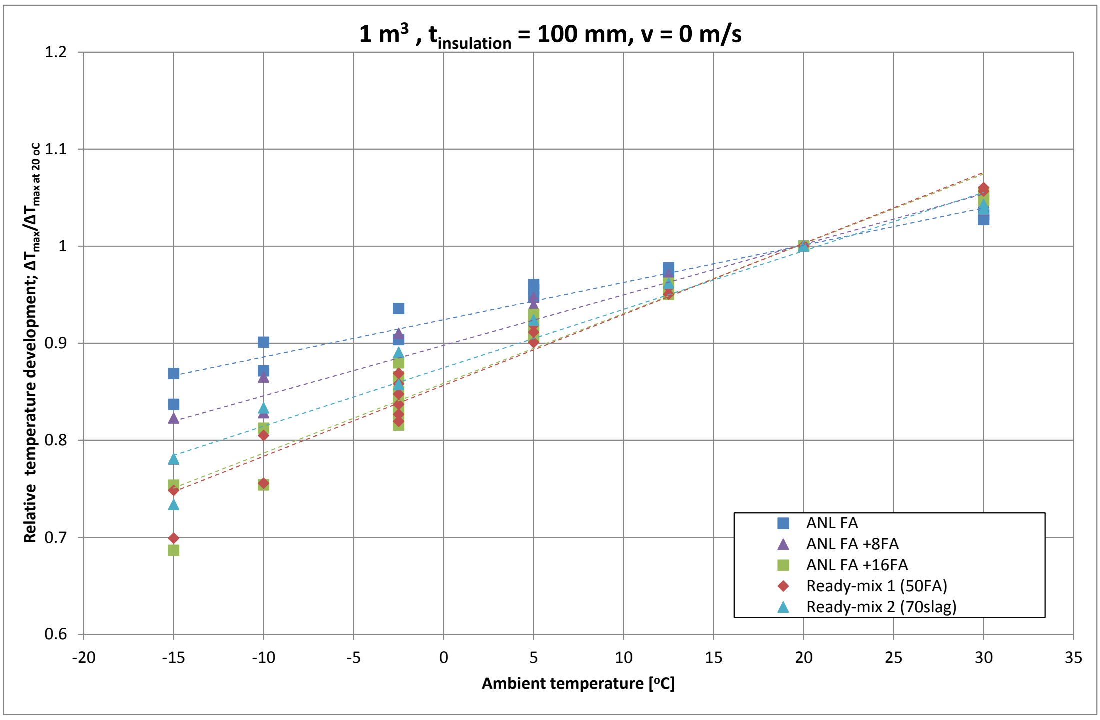

Figure 4.12 Relative temperature development versus ambient temperature, with a variety of initial concrete temperatures

The calculated ΔT_{max} trend lines (Figure 4.11 and Figure 4.13) are based on the average ΔT_{max} value for each of the relevant ambient temperatures. The trend lines are not parallel, hence one basic linear model representing all the concretes is established by the following formula:

$$\Delta T_{\max}(T_{amb}) = \Delta T_{\max 20} - 0.20 \cdot (20 - T_{amb}) \qquad \textit{Equation 4.1}$$

where ΔT_{max} is the maximum temperature increase in the core of the curing box, T_{amb} is the surrounding temperature, and ΔT_{max20} is the maximum temperature increase in the core of the curing box at a surrounding temperature of 20 °C

Equation 4.1 gives a linear relationship between ΔT_{max} and ambient temperature T_{amb}. The model is valid for all concretes and it is based on the concrete's maximum temperature increase at a surrounding temperature of 20 °C. The model constant was determined by using the method of least squares. The model (Equation 4.1*)* was fitted to the average ΔT_{max} value for each relevant ambient temperature for all of the four main concretes. As the concrete *Ready-mix 2* showed an unusual heat development, Figure 3.8, and the concrete anyhow is well within the «low-heat concrete»-limits, the ΔT_{max} analysis results for *Ready-mix 2* was not included when establishing *Equation 4.1*. In Figure 4.13, the average temperature increase ΔT_{max}, trend lines, as well as the defined model (Equation 4.1*)* are presented for the given concretes.

As can be seen from Figure 4.13, the established model gives very good agreement for concretes *ANL FA + 8FA* and *Ready-mix 1*. For concretes *ANL FA*, *ANL FA + 16FA* and *Ready-mix 2* there is a small deviation between model and analysis results, and the coefficient of variation (COV) is 2.6 %, 3.8 % and 8.3 %, respectively. This represents a deviation equal to 1.4 °C 1.4 °C and 2.4 °C, respectively, at an ambient temperature -10 °C.

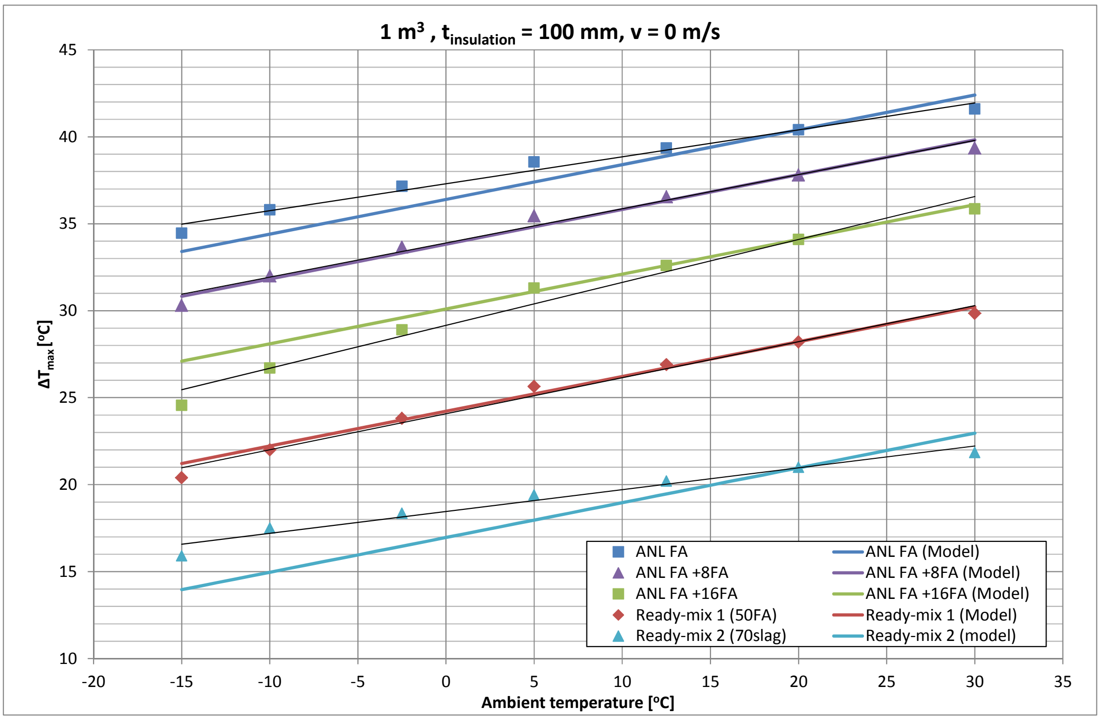

Figure 4.13 Ambient temperature versus average ΔT_{max} results, trend lines and model (Equation 4.1)

In Figure 4.14, the previously defined model (Equation 4.1) is implemented for the curing box case *«0.22 m³, $t_{insulation}$ = 200 mm»*. The model gives good agreement with concrete *ANL FA + 8FA*, *ANL FA + 16FA* and *Ready-mix 1 (50FA)*. The largest deviation occurs for *ANL*

FA with a COV equal to 3.7 %, which represents a deviation of 2 °C at an ambient temperature -10 °C.

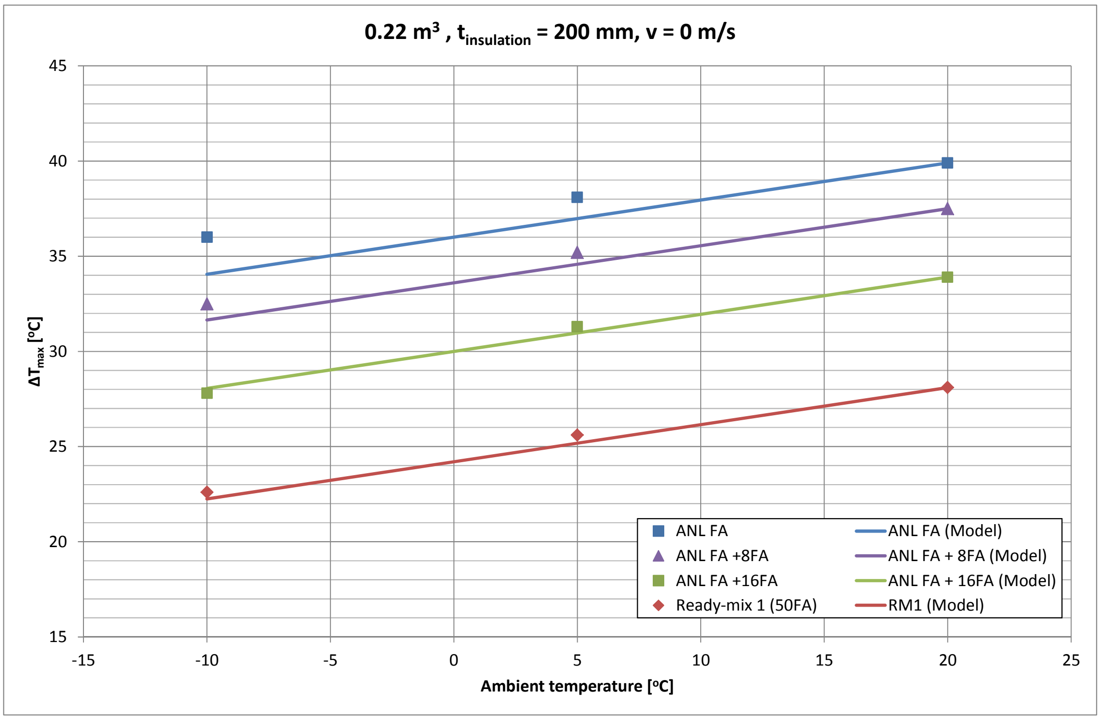

Figure 4.14 Ambient temperatures versus ΔT_{max} and model, 0.22 m^2, $t_{insulation}$ = 200 mm

An equivalent linear model for the curing box case «*1.0 m^2, $t_{insulation}$ = 200 mm*» is estimated to be:

$$\Delta T_{\max}(T_{amb}) = \Delta T_{\max 20} - 0.11 \cdot (20 - T_{amb}) \qquad \textit{Equation 4.2}$$

where ΔT_{max} is the maximum temperature increase in the core of the curing box, T_{amb} is the surrounding temperature, and ΔT_{max20} is the maximum temperature increase in the core of the curing box at a surrounding temperature of 20 °C

Equation 4.2 was determined in the same manner as Equation 4.1, by using the method of least squares. Equation 4.2 is however based on much less ΔT_{max} values than Equation 4.1. For example, the extreme values for T_{amb} = -15 °C and T_{amb} = 30 °C are not included. In Figure 4.15, the temperature increase ΔT_{max} and the defined model (Equation 4.2) are presented for the given concretes. The model gives very good agreement with the analysis results for all concretes. Maximum COV is 1.6 % and occurs for concrete *Ready-mix 1*. This represents a deviation between model and analysis result equal to 0.7 °C for an ambient temperature -10 °C.

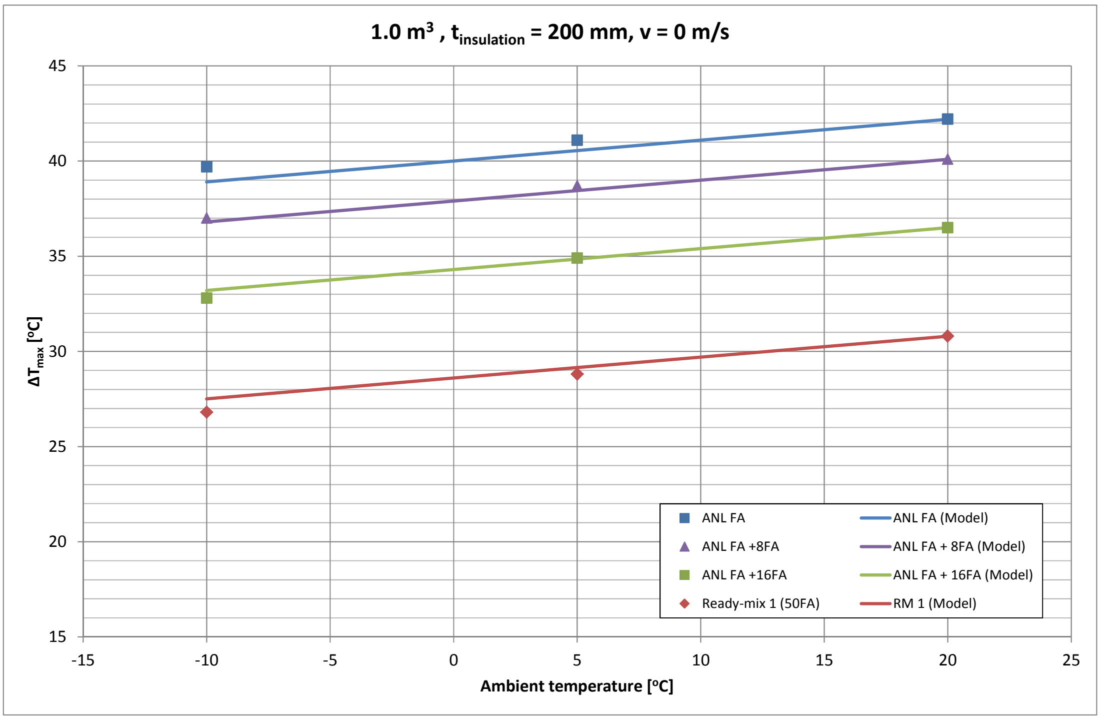

Figure 4.15 Ambient temperatures versus ΔT_{max} and estimated model, 1.0 m^2, $t_{insulation}$ = 200 mm

4.4 Wall

A series of analyses were performed with the aim to find out approximately what wall thickness each curing box variant represent (assuming normal plywood as formwork and average temperature for the wall, and curing box insulation thickness t = 100 mm), the results are presented in Table 4.7.

Table 4.7 ΔT_{max} and the appurtenant wall thickness that represents the given curing box

Size	ANL FA		ANL FA + 8FA		ANL FA + 16FA		Ready-mix 1 (50FA)	
[m^3]	ΔT_{max} [°C]	t [mm]	ΔT_{max} [°C]	t [mm]	ΔT_{max} [°C]	t [mm]	ΔT_{max} [°C]	t [mm]
1.00	40.4	1 430	37.8	1 500	34.1	1 540	28.2	1 510
0.51	38.9	1 250	36.1	1 300	32.5	1 360	26.8	1 310
0.22	36.9	1 050	33.9	1 100	29.9	1 130	24.6	1 070

From Table 4.7 it can be seen that what wall thickness a curing box represent is dependent both on the curing box size as well as the heat properties of the given concrete.

5 Conclusion

For all studied curing box alternatives, there seems to be an approximately linear correlation between ΔT_{max} and ambient temperature, where the slope of the trend line represents the curing box's sensitivity to the surrounding conditions. Among the studied curing box alternatives it is found, for instance, that the sensitivity of ΔT_{max} to the ambient temperature is about the same for a 0.2 m^3 curing box with 200 mm insulation and for a 1.0 m^3 curing box with 100 mm insulation. As expected, the largest 1.0 m^3 curing box with 200 mm insulation has the lowest sensitivity due to the ambient conditions, but there is still a difference of 5 ^oC in ΔT_{max} between the two extreme ambient temperature cases T = -15 ^oC and T = 30 ^oC. Hence, even when using the curing box with the least temperature sensitivity, it is still necessary to consider the ambient temperature. It can however be debated whether one curing box is more favourable than the other, as all seem to have an approximately linear correlation between ΔT_{max} and ambient temperature, and, thus, the ambient conditions can in principle be corrected for in all cases.

An extended series of analyses, with a variety of ambient temperatures and initial concrete temperatures, was conducted for the defined curing box reference case: *Size = 1.0 m*^{3}, $t_{insulation}$ *= 100 mm, v = 0 m/s*. The results show a rather linear correlation between ΔT_{max} and ambient temperature. One linear model for ΔT_{max} versus ambient temperature was established. The model gives good agreement with the analysis results for the concretes in question.

In addition, more as a curiosity, a series of analyses were performed with the aim to find out what wall thicknesses give a ΔT_{max} that is approximately equivalent to that of the various curing boxes with 100 mm insulation thicknesses. The results indicate that curing boxes with size 1.00 m^3, 0.51 m^3 and 0.22 m^3, represent wall thicknesses of about 1500 mm, 1300 mm, and 1100 mm. These are approximate numbers as it was also found that the relation to some extend was dependent on the hydration heat characteristics of the concrete.

References

Kjellmark G., Klausen A. and Kanstad T. (2013): *Mechanical properties and calculation of model parameters for concrete with variable fly ash content.* DRAFT COIN Project report, FA 3.1, Trondheim, Norway, 2013

JEJMS Concrete AB (2009-2012): *ConTeST Pro (Now CrackTeSt COIN) Manual*. Luleå, Sweden, 2008

Microsoft Office (2010): *Microsoft Excel*. Version: 14.0.6123.5001, 2010

Statens Vegvesen (2013): http://www.vegvesen.no/Europaveg/e6ost/Strindheimtunnelen

SINTEF test report (2011): *Tunnel Møllenberg – Young low-heat concrete 100% FA*, Documentation of properties for cast concrete (in Norwegian). Report 33409/A. Trondheim

Kristiansen B./AF Gruppen (2013): Personal E-mail received 25.11.2013 giving temperature registrations in a curing box cast with a concrete with CEM III/B

TNO DIANA BV (2010): *User's Manual -- Release 9.4.3*

Appendix

APPENDIX A BOUNDARY CONVECTION

The boundary convection coefficients in the current analyses are calculated from the following equations.

From [JEJMS Concrete AB, 2008]:

At external boundaries, where the surrounding medium is air, the heat transfer coefficient is described by:

$$h_{free} = \begin{cases} 5.6 + 3.95\text{v} & \text{for } v < 5 \text{ m/s} \\ 7.8\text{v}^{0.78} & \text{for } v > 5 \text{ m/s} \end{cases}$$

where h_{free} = heat transfer coefficient for a free surface surrounded by air, W/m^{2}K
v = air velocity, m/s

The heat flow from the external boundary to the surroundings may at several layers of different boundary materials be described as a (combined) heat transfer coefficient according to:

$$h_{surf} = \left(\frac{1}{h_{free}} + \sum_i \frac{l_i}{k_i} \right)^{-1}$$

where l_i = thickness of the i:th boundary material, m
k_i = heat conductivity of the i:th boundary material, W/mK

$$\frac{1}{h_{free}} = \text{alt.} \begin{cases} \text{with } h_{free} \text{according to above for the cases in contact with air} \\ 0 \text{ for the cases in contect with something else than air} \end{cases}$$

Different boundary conditions cause different boundary convections. In the current analyses, both two different insulations thicknesses, as well as two different wind speeds, are used. The insulation thicknesses of the curing boxes are t = 100 mm and t = 200 mm. while the two different wind speeds chosen are v = 0 m/s and v = 5 m/s.

Additionally, a 12 mm layer of plywood, k = 0.14 W/mK, is assumed.

The heat convection for the chosen insulation material, 50 mm Sundolitt XPS 500 (http://www.sundolitt.no/sundolitt/produkter/sundolitt-xps-standard/sundolitt-xps-500) is set to 0.034 W/mK, thus follows:

t = 100 mm. v = 0 m/s:

$$\frac{1}{h_{free}} = \frac{1}{5.6}$$

$$h_{surf} = \left(0.179 + \frac{0.012}{0.14} + \frac{0.10}{0.034}\right)^{-1} = \frac{1}{3.205} = 0.312$$

t = 100 mm. v = 5 m/s;

$$\frac{1}{h_{free}} = \frac{1}{5.6 + 3.95 \cdot 5} = 0.0394$$

$$h_{surf} = \left(0.0394 + \frac{0.012}{0.14} + \frac{0.10}{0.034}\right)^{-1} = \frac{1}{3.066} = 0.326$$

t = 200 mm. v = 0 m/s:

$$\frac{1}{h_{free}} = \frac{1}{5.6}$$

$$h_{surf} = \left(0.179 + \frac{0.012}{0.14} + \frac{0.20}{0.034}\right)^{-1} = \frac{1}{6.147} = 0.163$$

t = 200 mm. v = 5 m/s:

$$\frac{1}{h_{free}} = \frac{1}{5.6 + 3.95 \cdot 5} = 0.0394$$

$$h_{surf} = \left(0.0394 + \frac{0.012}{0.14} + \frac{0.20}{0.034}\right)^{-1} = \frac{1}{6.007} = 0.166$$

The bottom of the curing box, i.e. one of six sides, may not be exposed to air. Hence, the bottom of the curing box obtains the following heat conduction:

t = 100 mm. v = 0 m/s. bottom curing box:

$$\frac{1}{h_{free}} = 0$$

$$h_{surf} = \left(0 + \frac{0.012}{0.14} + \frac{0.10}{0.034}\right)^{-1} = \frac{1}{3.027} = 0.330$$

t = 200 mm. v = 0 m/s. bottom curing box:

$$\frac{1}{h_{free}} = 0$$

$$h_{surf} = \left(0 + \frac{0.012}{0.14} + \frac{0.20}{0.034}\right)^{-1} = \frac{1}{5.968} = 0.168$$

Hence it follows that for the curing box «t = 100mm and v = 0», 16.7 % of the boundaries has a heat convection increase of 5.8 %. This is considered neglectable, and thus all the sides of the curing box are applied the same heat convection coefficient.

APPENDIX B HEAT DEVELOPMENT

ANL FA:

Adiabatic temperature and isothermic heat SKANSKA

(v 2.8 ss 06-02-2012)

Concrete parameters

Temp. trans. coeff.	0,0206
Density	2385
Heat capacity (fresh)	1,01
Heat capacity (hardened)	1,01
Cement content	387
Set time	8,8
A - set time	31515
B - set time	270
A - hydration	31515
B - hydration	270
Adia. start temperature	20

Temp. trans. coeff.

dQ/dm	0,05
m>	250
m<	300

Heat function

m-limit	345
Q_∞	295
τ	19,98
α	1,07
R^2	0,9738
$\Sigma\Delta Q$	7308

Heat polygon

Reference heat [kJ/kg cem]	*Corresp. maturity [h]*
0	0,0
5	5,6
10	7,6
20	9,3
30	10,5
40	11,6
60	13,5
80	15,5
100	17,3
120	19,6
140	23,2
160	29,2
180	38,8
200	52,2
210	60,3
220	69,5
240	91,8
260	135,0
270	179,7

Adapt the temperature transmission coefficient: **<Ctrl> t**
Adapt the heat function: **<Ctrl> h**

$$Q = Q_\infty \cdot e^{\left(-\frac{\tau}{M}\right)^\alpha}$$

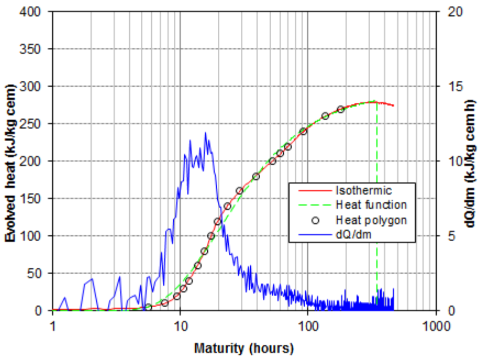

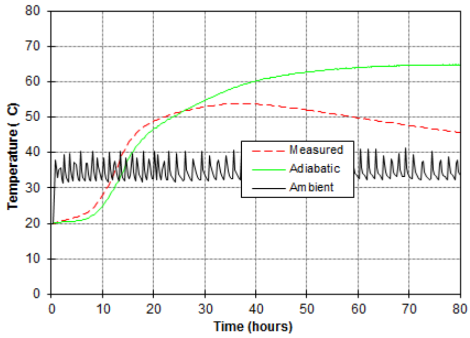

Project

Name	COIN P3.1 serie_master Gøran
Test id	Kanal 2_ANL FA
Perf. by	Gunrid Kjellmark, SINTEF Byggforsk
Date	15.05.2013

ANL FA + 8FA:

Adiabatic temperature and isothermic heat

SKANSKA

(v 2.8 ss 06-02-2012)

Concrete parameters

Temp. trans. coeff.	0,0240
Density	2377
Heat capacity (fresh)	1,01
Heat capacity (hardened)	1,01
Cement content	382
Set time	9,3
A - set time	32874
B - set time	399
A - hydration	32874
B - hydration	399
Adia. start temperature	20

Temp. trans. coeff.

dQ/dm	0,075
m>	250
m<	300

Heat function

m-limit	330
Q_∞	296
τ	25,69
α	0,92
R^2	0,9720
$\Sigma\Delta Q$	16009

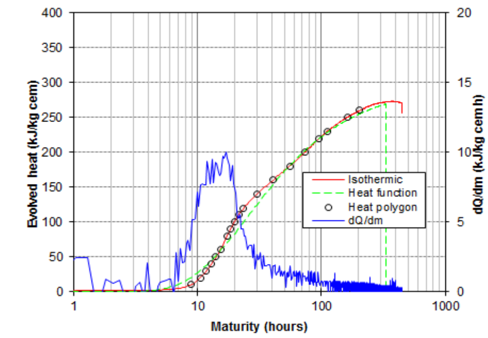

Heat polygon

Reference heat [kJ/kg cem]	Coresp. maturity [h]
0	0,0
10	8,9
20	10,5
30	11,8
40	12,9
50	14,1
60	15,2
80	17,3
90	18,5
100	19,7
110	21,4
120	23,5
140	30,2
160	40,5
180	55,3
200	73,4
220	95,8
230	111,0
250	161,0
260	203,8

Adapt the temperature transmission coefficient: **<Ctrl> t**
Adapt the heat function: **<Ctrl> h**

$$Q = Q_\infty \cdot e^{\left(-\frac{\tau}{M}\right)^{\alpha}}$$

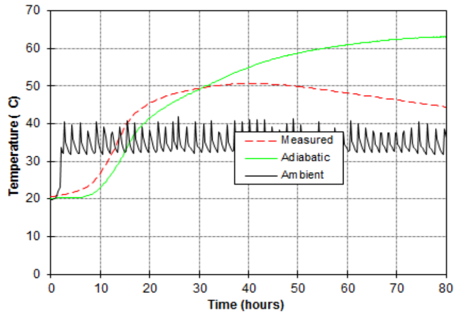

Project

Name	COIN P3.1 serie_master Gøran
Test id	Kanal 3_ANL FA + 8FA
Perf. by	Gunrid Kjellmark, SINTEF Byggforsk
Date	15.05.2013

ANL FA + 16FA:

Adiabatic temperature and isothermic heat

SKANSKA

(v 2.8 ss 06-02-2012)

Concrete parameters

Temp. trans. coeff.	0,0265
Density	2377
Heat capacity (fresh)	1,01
Heat capacity (hardened)	1,01
Cement content	377
Set time	10,2
A - set time	36421
B - set time	104
A - hydration	36421
B - hydration	104
Adia. start temperature	20

Temp. trans. coeff.

dQ/dm	0,1
m>	250
m<	300

Heat function

m-limit	320
Q_∞	302
τ	32,64
α	0,76
R^2	0,9792
$\Sigma\Delta Q$	11900

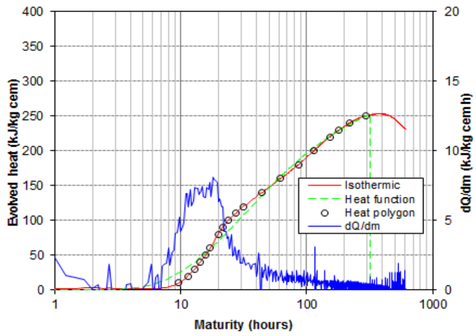

Heat polygon

Reference heat [kJ/kg cem]	Coresp. maturity [h]
0	0,0
10	9,6
20	11,4
30	12,9
40	14,3
50	15,7
60	17,1
80	19,7
90	21,4
100	23,8
110	27,1
120	31,5
140	44,0
160	62,0
180	85,5
200	113,7
220	152,2
230	181,0
240	220,1
250	293,4

Adapt the temperature transmission coefficient: **<Ctrl> t**

$$Q = Q_\infty \cdot e^{\left(-\frac{\tau}{M}\right)^{\alpha}}$$

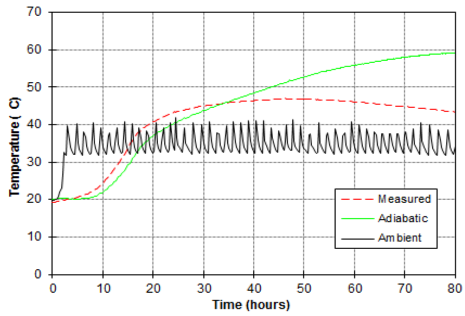

Project

Name	COIN P3.1 serie_master Gøran
Test id	Kanal 4_ANL FA + 16FA
Perf. by	Gunrid Kjellmark, SINTEF Byggforsk
Date	15.05.2013

Ready-mix 1 (50FA):

Adiabatic temperature and isothermic heat SKANSKA

(v 2.8 ss 06-02-2012)

Concrete parameters

Temp. trans. coeff.	0,0046
Density	2375
Heat capacity (fresh)	1,03
Heat capacity (hardened)	1,03
Cement content	332
Set time	12
A - set time	35000
B - set time	0
A - hydration	35000
B - hydration	0
Adia. start temperature	20

Temp. trans. coeff.

dQ/dm	0,05
m>	430
m<	450

Heat function

m-limit	450
Q_∞	277
τ	25,68
α	0,89
R^2	0,9799
ΣΔQ	15891

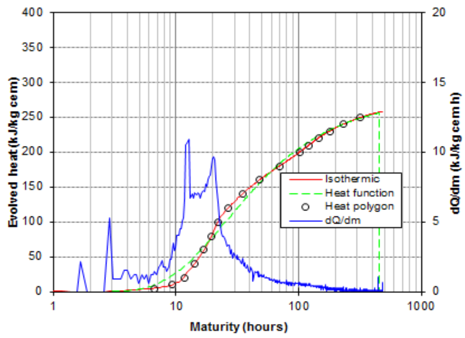

Heat polygon

Reference heat [kJ/kg cem]	Corresp. maturity [h]
0	-0,3
5	6,6
10	9,3
20	11,6
40	14,1
60	16,9
80	19,4
100	21,7
120	26,6
140	34,6
160	47,5
180	69,4
200	101,4
210	120,9
220	144,3
230	178,1
240	230,4
250	319,5

Adapt the temperature transmission coefficient: <Ctrl> t

$$Q = Q_\infty \cdot e^{\left(-\frac{\tau}{M}\right)^{\alpha}}$$

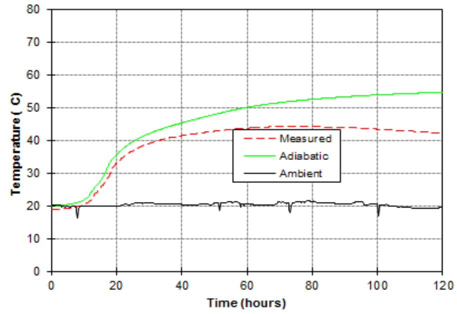

Project

Name	COIN P3.1 serie_master Gøran
Test id	Kanal 2_ANL FA
Perf. by	Gunrid Kjellmark, SINTEF Byggforsk
Date	15.05.2013

Ready-mix 2 (70slag):

Adiabatic temperature and isothermic heat SKANSKA

(v 2.8 ss 06-02-2012)

Concrete parameters

Temp. trans. coeff.	0,0157
Density	2440
Heat capacity (fresh)	1,01
Heat capacity (hardened)	1,01
Cement content	392
Set time	12
A - set time	35000
B - set time	0
A - hydration	35000
B - hydration	0
Adia. start temperature	20

Temp. trans. coeff.

dQ/dm	0,1
m>	110
m<	130

Heat function

m-limit	150
Q_∞	162
τ	19,08
α	1,18
R^2	0,9936
ΣΔQ	5196

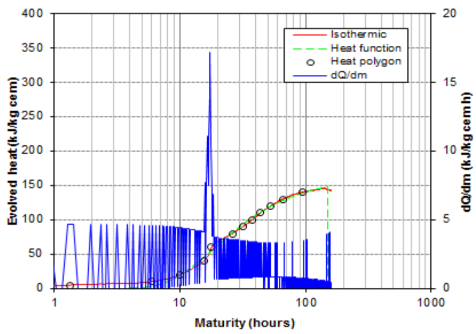

Heat polygon

Reference heat [kJ/kg cem]	Corresp. maturity [h]
0	0,0
5	1,3
10	5,9
20	10,0
40	15,7
60	17,8
80	26,2
90	31,9
100	37,6
110	43,7
120	52,7
130	66,3
140	94,5

Adapt the temperature transmission coefficient: <Ctrl> t

$$Q = Q_\infty \cdot e^{\left(-\frac{\tau}{M}\right)^{\alpha}}$$

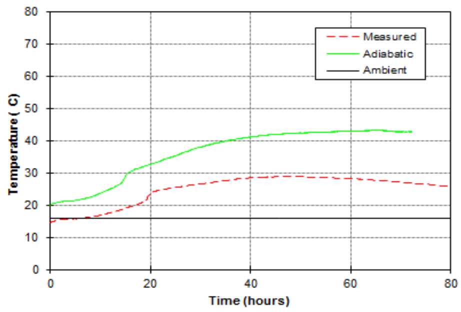

Project

Name	Ready-mix 2 (70slag)
Test id	
Perf. by	Anja Klausen
Date	15.11.2013

APPENDIX C READY-MIX 2 (70SLAG)

Mix design for Ready-mix 2 (70slag):

	Ready-mix 2 (70slag) [kg/m^3]
CEMIII/B42,5N-LHHSNA	380.5
FA_{cem}	0
FA_{added}	0
Silica	11.8
Free water	97.3
Sand 0–4N.2	456.5
Sand 0–4	456.5
Gravel 4–8	212.5
Gravel 8–16	420.5
Gravel 16–22	399.5
Admixture	3.8

Material coefficients for Ready-mix 2 (70slag):

		Ready-mix 2 (70slag)
Density	[kg/m^3]	2 440
Th. conductivity	[W/mK]	2.2
Heat capacity	[kJ/m^{3}K]	2 464
Arrhenius	[K]	4 210*)

*) *Arrhenius constant is constant for all temperatures, and based on the activation energy at 20 °C.*

Sandnes Betong AS - Anlegg 1 **Blandelog**

4323 Sandnes
Tel.:51685120
Fax.:
W..:www.sandnesbetong.no @..:post@sandnesbetong.no

Følgeseddel opplysninger

Flgsdl: **43137680** Dato: **24.04.2013 12:17:11**
Resept: **3511M40 B35 D22 M40 CEM IIIB**
K/P: **200221 - Diverse ikke faktura / 73 - Prøvestøp - Cem IIIB**
Type: **Almindelig resept**
Flg m³: **2,00/(2,000)** Prod m³: **2,01**

Bl.mester:
Synkmål: **150 mm**
Standard: **Ingen**
Satse: **1** Satsstr: **2,01**

Vekt sats opplysninger

Materiale (Ønsket mat/silo i 1. sats fra resepten)	Silo	Sats 1 Ønsket	Sats korr.	Oppnådd	Afvikelse %	FUKT %	Vanninnhold	Less Ønsket	Oppnådd	Afvikelse %
Pukk 16-22	1	799		788	-1,31	0,00	0,00	799	788	-1,31
Pukk 4-8	6	425		427	0,52	0,50	2,11	425	427	0,52
Pukk 8-16	4	841		838	-0,42	0,50	4,15	841	838	-0,42
Støpesand 0-4vN.2	3	913		915	0,19	5,50	47,38	913	915	0,19
Støpesand 0-4vN	5	913		915	0,19	5,50	47,38	913	915	0,19
Tilslag total		3891		3882	**-0,21**			3891	3882	**-0,21**
CEMIII/B42,5N-LHHSNA	3	760,9		762,3	**0,18**		0,00	760,9	762,3	**0,18**
Silica	1	23,5		24,2	**2,93**		0,00	23,5	24,2	**2,93**
Kaldt vann	1	194,67		193,22	-0,74		193,22	194,67	193,22	-0,74
Varmt Vann	2	0,00		0,00	0,00		0,00	0,00	0,00	NAN
Vann total		194,67		193,22	**-0,74**			194,67	193,22	**-0,74**
Sika Retarder	5	1,412		1,380	**-2,28**		1,03	1,412	1,380	**-2,28**
Sika AER S	4	1,569		1,600	**1,96**		1,59	1,569	1,600	**1,96**
ViscoCrete RMC -630	3	4,706		4,689	**-0,38**		3,84	4,706	4,689	**-0,38**
Ekstra vann				9,0			9,00		9,0	
Total Kg		**4878**		**4879**			**309,72**	**4878**	**4879**	

Utefinerede Kg Satsnr.	Tilslag 1	Sement 1	Vann 1	Tilset. 1	Silica 1
1	2,14	0,73	-0,92	-0,05	-1,24
Ialt	2,14	0,73	-0,92	-0,05	-1,24

Øvrige sats opplysninger

Satsnr.	Blander Blandetid	Efter spedvann antå	Wattmeter	Blander	Temperatur
Ønsket	90,0				
1	353,0	210,4	29,0	Blander 1	

Øvrige less opplysninger

	Ønsket	Oppnådd	Afvikelse
VC-Forhold	0,385	0,394	0,009
Totale kg i less	4878	4879	0,0
Frit vann	302,00	309,72	2,6 %
Ekv.cem.mengde	784,42	786,49	0,3 %

~~Slump~~
+ 1,5 l Sika Aer S 1:19
+ 0,5 l RMC 630
i bilen.

Utskrevet d. 24.04.2013 14:21:49 Utskrift nr. 574
System 4009, Build 1.13.26

Side 1 Av 1

APPENDIX D DIANA FILES

Input file, 1.0 m^3 and winter condition:

```
 ! iDIANA Version 9.4.3 Release 02
 ! Installed for : Diana-Teaching
 ! History file for model : Herdekasse
 ! Session started at 14 NOV 2013 09:11:26

!Units and filname-output
 FEMGEN HK_1
 PROPERTY FE-PROG DIANA HTSTAG_3D  ; YES
 UTILITY SETUP UNITS LENGTH MILLIMETER
 UTILITY SETUP UNITS MASS KILOGRAM
 UTILITY SETUP UNITS FORCE NEWTON
 UTILITY SETUP UNITS TIME SEC
 UTILITY SETUP UNITS TEMP CELSIUS
 UTILITY SETUP UNDO ON
 UTILITY SETUP BINSET OFF
 MESHING OPTIONS CHECK STRUCTURED OFF
 UTILITY SETUP OPTIONS ANALYSIS SOLVER-COMMAND diana_w

!Geometry
 GEOMETRY POINT COORD P1 0 0 0
 GEOMETRY POINT COORD P2 1000
 GEOMETRY POINT COORD P3 1000 1000
 GEOMETRY POINT COORD P4 0 1000

 GEOMETRY SURFACE 4POINTS S1 P1 P2 P3 P4

!meshing
 MESHING DIVISION S1 8 8

 CONSTRUCT SET TVERR1 APPEND S1
 GEOMETRY SWEEP TVERR1 TVERR2 TRANSLATE TR1 0 0 -1000

 MESHING DIVISION L9 8
 MESHING DIVISION L10 8
 MESHING DIVISION L11 8
 MESHING DIVISION L12 8

 MESHING TYPES ALL NONE

 MESHING TYPES B1 CHX60

  VIEW GEOMETRY ALL
 LABEL GEOMETRY LINES

!GENERATING MESH
 MESHING GENERATE

 EYE FRAME
 VIEW MESH B1 GREEN

!DEFINITION OF SURFACES/BOUNDARIES;
!sURF = ALL SURFACES WITH BOUNDARIES
!SURF1 = SIDES AND TOP
```

```
!SURF2 = BOTTOM

  CONSTRUCT SET SURF1 APPEND S1 S2 S4 S5 S6
  CONSTRUCT SET SURF2 APPEND S3
  CONSTRUCT SET SURF APPEND SURF1 SURF2

!DEFINITION OF BOUNDARIES,
!BOUND = ALL CONVECTION BOUNDARIES
!CONV1 = FREE SIDES
!CONV2 = BOTTOM
!GENERATING NEW SURFACES FOR CONVECTION ELEMENTS

  CONSTRUCT SPACE TOLERANCE OFF
  CONSTRUCT SET OPEN BOUND
  GEOMETRY COPY SURF1 FREE TRANSLATE 0 0 0
  GEOMETRY COPY SURF2 BOTTOM TRANSLATE 0 0 0
  CONSTRUCT SET CLOSE

!REDUCING NODES DUE TO LINEAR SURFACE FLOW ELEMENT
  MESHING DIVISION FACTOR BOUND 0.5
  MESHING TYPES BOUND BQ4HT

!GENERATING MESH FOR SLAB AND WALLS
  MESHING GENERATE BOUND

!MERGING DOUBLE-NODES
  MESHING MERGE ALL

  CONSTRUCT SPACE TOLERANCE ON

!BOUNDARY CONSTRAINTS
  PROPERTY BOUNDARY CONSTRAINT P1 x Y
  PROPERTY BOUNDARY CONSTRAINT P5 x Y
  PROPERTY BOUNDARY CONSTRAINT P2 Y
  PROPERTY BOUNDARY CONSTRAINT P6 Y

!MATERIAL PROPERTIES
  PROPERTY MATERIAL MA1 EXTERNAL EXTERNAL "MA1_FA.DAT"
  PROPERTY MATERIAL MA2 EXTERNAL EXTERNAL "MA_10_0.DAT"
  PROPERTY MATERIAL MA3 EXTERNAL EXTERNAL "MA_10_0.DAT"

  PROPERTY ATTACH B1 MA1
  PROPERTY ATTACH FREE MA2
  PROPERTY ATTACH BOTTOM MA3

!BOUNDARY CONDITIONS, INITIAL TEMPERATURE, LOADS
!The EXTTEMP load class defines an external temperature for boundary elements

   PROPERTY LOADS EXTTEMP 1 FREE -10
  PROPERTY LOADS EXTTEMP 2 BOTTOM -10
  VIEW MESH OFF

  PROPERTY INITIAL INITEMP ALL 15.
```

Materials file, ANL FA:

```
ADIAB    0 20.00
         7200 20.10
         18000 20.68
         28800 21.96
         39600 26.35
         50400 34.04
         61200 42.08
         72000 46.66
         82800 49.39
         93600 51.78
         104400 54.06
         115200 56.10
         126000 57.96
         136800 59.44
         147600 60.64
         158400 61.43
         169200 62.20
         180000 62.84
         190800 63.28
         201600 63.70
         212400 64.08
         223200 64.29
         234000 64.52
         244800 64.63
         255600 64.71
         266400 64.79
         288000 64.84
         309600 64.86
         331200 64.87
         1209600 64.90
  DENSITY     2390e-9
  CONDUC      2.2e-6
  CAPACI      2414e-9
  ARRHEN      3792.
  YOUNG       1
  THERMX      8.7E-6
  POISON      0.2
  EQUAGE      ARRTYP
```

Materials file, t = 100 mm, v = 0 m/s;

```
CONVEC      0.312E-9
TIME        0.            1.21E6
CONVTT      0.312E-9      0.312E-9
```

Analysis file:

```
*FILOS
INITIA
*INPUT
*HEATTR
BEGIN INITIA
  BEGIN NONLIN
    HYDRAT DGRINI=0.0001
    EQUAGE EQAINI=0.1
  END NONLIN
  TEMPER INPUT
END INITIA
BEGIN EXECUTE
  ALPHA=0.67
  SIZES 1800(6) 3600(20) 7200(20) 14400(12) 43200 (8) 86400 (6)
    BEGIN NONLIN
      ITERAT MAXITE=10
      HYDRAT ITERAT
    END NONLIN
END EXECUTE
BEGIN OUTPUT FEMVIE FILE="TEMPFLOW"
  TEMPER
  REACTI
  EQUAGE
END OUTPUT
*NONLIN
*END
```

Result file:

```
RESULTS LOADCASE TR1 1 TO TR1 72
RESULTS NODAL PTE....S PTE

UTILITY TABULATE PRINTFILE OPEN temperatur_midt.txt
PRESENT GRAPH NODE 346
UTILITY TABULATE PRINTFILE CLOSE
```

SINTEF Building and Infrastructure is the third largest building research institute in Europe. Our objective is to promote environmentally friendly, cost-effective products and solutions within the built environment. SINTEF Building and Infrastructure is Norway's leading provider of research-based knowledge to the construction sector. Through our activity in research and development, we have established a unique platform for disseminating knowledge throughout a large part of the construction industry.

COIN – Concrete Innovation Center is a Center for Research based Innovation (CRI) initiated by the Research Council of Norway. The vision of COIN is creation of more attractive concrete buildings and constructions. The primary goal is to fulfill this vision by bringing the development a major leap forward by long-term research in close alliances with the industry regarding advanced materials, efficient construction techniques and new design concepts combined with more environmentally friendly material production.